

Cite this: *RSC Adv.*, 2019, 9, 24117

# Synthesis, structural studies and biological properties of some phosphono-perfluorophenylalanine derivatives formed by $S_NAr$ reactions†‡

Joanna Kwiczak-Yiğitbaşı,<sup>ab</sup> Jean-Luc Pirat,<sup>b</sup> David Virieux,<sup>id b</sup> Jean-Noël Volle,<sup>\*b</sup> Agnieszka Janiak,<sup>id a</sup> Marcin Hoffmann,<sup>id a</sup> Jakub Mrzygłód,<sup>a</sup> Dariusz Wawrzyniak,<sup>c</sup> Jan Barciszewski<sup>id cd</sup> and Donata Pluskota-Karwatka<sup>id \*a</sup>

Several novel phosphono-perfluorophenylalanine derivatives, as mimetics of phenylalanine, were synthesized by subjecting diethyl (2-(perfluorophenyl)-1-(phenylamino)ethyl)-phosphonate to  $S_NAr$  reactions with different types of nucleophiles such as thiols, amines and phenols. The structure of the products was confirmed using spectroscopic and spectrometric techniques. For two compounds X-ray single crystal diffraction analysis and DFT investigations were performed providing information in regard to the preferable conformation, hydrogen bonds and other interactions. The antiproliferative potency of some of the new phosphono-perfluorophenylalanine derivatives obtained as well as representatives of previously synthesized perfluorophenyl phosphonate analogues of phenylalanine was studied on selected glioma cell lines. Preliminary evaluation of the compounds drug likeness was examined with respect to Lipinski's and Veber's rules, and showed that they meet the criteria perfectly. MTT (3-(4,5-dimethyl-2-thiazolyl)-2,5-diphenyl-2H-tetrazolium bromide) assay results demonstrated that the compounds exhibit moderate activity against the glioblastoma multiforme cell lines (T98G and U-118 MG). Moreover most of the studied  $S_NAr$  reaction products displayed significantly higher inhibitory activity against both cancer cell lines than the parent diethyl (2-(perfluorophenyl)-1-(phenylamino)ethyl) phosphonate.

Received 26th May 2019

Accepted 16th July 2019

DOI: 10.1039/c9ra03982a

rsc.li/rsc-advances

## 1. Introduction

Chemistry of  $\alpha$ -aminophosphonates has played a significant role in the development of organophosphorus compounds, and still remains a field of great interest.<sup>1–3</sup> As structural analogues of  $\alpha$ -amino acids,  $\alpha$ -aminophosphonates have found application in organic and medicinal chemistry,<sup>4</sup> mainly due to their anticancer,<sup>5–9</sup> antiviral<sup>10</sup> and antibacterial<sup>11,12</sup> activities. Moreover, phosphonates represent classical phosphate bioisosters, in which the labile O–P bond is replaced by an enzymatically

and chemically stable C–P bond. This change makes  $\alpha$ -amino-phosphonates structurally similar to phosphate esters or anhydrides, yet increases their stability under physiological and chemical conditions.<sup>13,14</sup> Also, the tetrahedral geometry on the phosphorus atom mimics the transition state of peptide hydrolysis thus,  $\alpha$ -aminophosphonates can act as enzyme inhibitors.<sup>15–17</sup>

Among  $\alpha$ -aminophosphonates, the fluorinated ones constitute a particularly important group of compounds. The incorporation of fluorine atoms in the structure of  $\alpha$ -aminophosphonates provides access to more lipophilic molecules, which often exhibit better biological activities than the parent compounds.<sup>18,19</sup> What is more, the presence of fluorine and phosphorus atoms in the  $\alpha$ -aminophosphonates structure gives us a chance to use <sup>19</sup>F and <sup>31</sup>P NMR spectroscopy to follow the location and to study the molecular interactions in biological systems.<sup>20,21</sup>

Introduction of fluorine has also become an important strategy in protein biochemistry. Fluorinated amino acids serve as powerful tools for exploring polar  $\pi$ -interactions in proteins,<sup>22,23</sup> and enabling novel recognition mechanisms for protein design.<sup>24–26</sup> Heavily fluorinated aromatic residues are

<sup>a</sup>Adam Mickiewicz University in Poznań, Faculty of Chemistry, Umultowska 89b, 61-614 Poznań, Poland. E-mail: donatap@amu.edu.pl

<sup>b</sup>AM2N, UMR 5253, ICGM, ENSCM, 8 Rue de L'Ecole Normale, 34296 Montpellier Cedex 5, France. E-mail: jean-noel.volle@enscm.fr

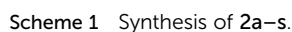
<sup>c</sup>Institute of Bioorganic Chemistry, Polish Academy of Sciences, Noskowskiego 12/14, 61-704 Poznań, Poland

<sup>d</sup>NanoBioMedical Center of Adam Mickiewicz University, Umultowska 85, 61-614, Poznań, Poland

† Dedication to Professor Henryk Koroniak in honour of his 70th birthday.

‡ Electronic supplementary information (ESI) available. CCDC 1912530 and 1912531. For ESI and crystallographic data in CIF or other electronic format see DOI: 10.1039/c9ra03982a

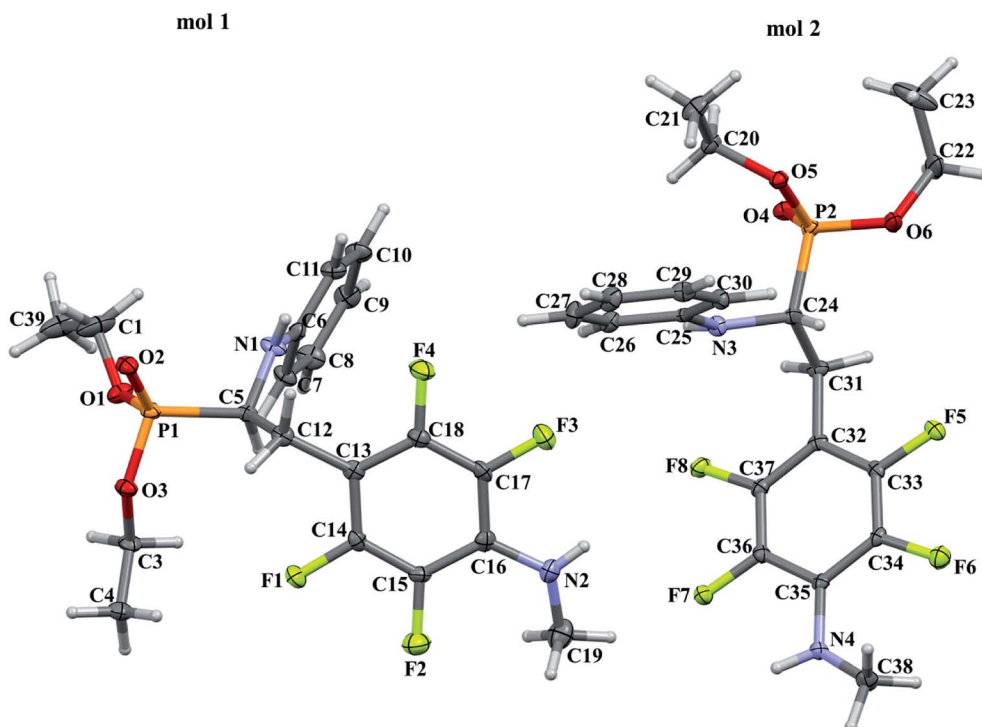
As part of our investigations, we have recently reported a convenient synthetic method for the preparation of a series of phosphonate analogues of phenylglycine, homophenylalanine, and phenylalanine that differ in the number and position of fluorine atoms in the phenyl ring.<sup>33,34</sup> These studies were supported by single-crystal X-ray diffraction analysis and quantum chemical calculations that provided information concerning the conformational preferences both in the solid and isolated states. Indeed, some of the obtained aminophosphonates underwent intramolecular  $S_NAr$  reactions yielding indolinyolphosphonates as minor products.<sup>33</sup> Since  $S_NAr$  reaction is an attractive and effective way for modifying structure of fluorinated aromatic compounds, we decided to study the ability of the synthesized  $\alpha$ -aminophosphonates to undergo such a transformation. It gave us a chance to obtain a library of diversely substituted  $\alpha$ -aminophosphonates and opened a new perspectives to seek for original bioactive molecules. Therefore in this paper we describe the synthesis of *para* substituted derivatives of diethyl (2-(perfluorophenyl)-1-(phenylamino)ethyl)phosphonate **1a** (Scheme 1) as well as results of their X-ray and DFT studies. Structural variations on products were achieved by subjecting the phenylalanine analogue **1a** to reactions with various nucleophiles, *i.e.* thiols, amines and phenols (Scheme 1).



Entry	Compound	Nucleophile	Conditions	Yield [%]
1	<b>2a</b>	C <sub>6</sub> H <sub>5</sub> SH	TRIS, DMF, rt, 2 h	87
2	<b>2b</b>	4-CH <sub>3</sub> C <sub>6</sub> H <sub>4</sub> SH		89
3	<b>2c</b>	3,5-(CH <sub>3</sub> ) <sub>2</sub> C <sub>6</sub> H <sub>3</sub> SH		81
4	<b>2d</b>	4-CH <sub>3</sub> OC <sub>6</sub> H <sub>4</sub> SH		95
5	<b>2e</b>	3-CH <sub>3</sub> OC <sub>6</sub> H <sub>4</sub> SH		84
6	<b>2f</b>	3-NH <sub>2</sub> C <sub>6</sub> H <sub>4</sub> SH		76
7	<b>2g</b>	4-BrC <sub>6</sub> H <sub>4</sub> SH		86
8	<b>2h</b>	C <sub>6</sub> H <sub>5</sub> CH <sub>2</sub> SH		65
9	<b>2i</b>	CH <sub>3</sub> (CH <sub>2</sub> ) <sub>8</sub> CH <sub>2</sub> SH		37
10	<b>2j</b>	<i>N</i> -acetyl-L-cysteine methyl ester	DMSO, 80 °C, 3 h	71
11	<b>2k</b>	CH <sub>3</sub> NH <sub>2</sub>		71
12	<b>2l</b>	CH <sub>3</sub> (CH <sub>2</sub> ) <sub>2</sub> NH <sub>2</sub>		74
13	<b>2m</b>	CH <sub>3</sub> (CH <sub>2</sub> ) <sub>3</sub> NH <sub>2</sub>		60
14	<b>2n</b>	CH <sub>2</sub> =CHCH <sub>2</sub> NH <sub>2</sub>		65
15	<b>2o</b>	C <sub>6</sub> H <sub>5</sub> CH <sub>2</sub> NH <sub>2</sub>	K <sub>2</sub> CO <sub>3</sub> , DMF, 80 °C, 24 h	63
16	<b>2p</b>	C <sub>6</sub> H <sub>5</sub> OH		68
17	<b>2q</b>	4-CH <sub>3</sub> OC <sub>6</sub> H <sub>4</sub> OH		48
18	<b>2r</b>	4-ClC <sub>6</sub> H <sub>4</sub> OH		56
19	<b>2s</b>	3-NO <sub>2</sub> C <sub>6</sub> H <sub>4</sub> OH		48

Reaction of **1a** with a large excess of alkylamine in DMSO after 3 hours of heating at 80 °C gave aryl aminophosphonates **2k–o** in yields ranging from 60 to 74% (Table 1, entries 11–15). Progress of the reactions was monitored by <sup>19</sup>F NMR, and after 3 hours a total conversion of the starting  $\alpha$ -aminophosphonate was generally observed.

Different phenols were consecutively used as nucleophiles. The expected products were obtained in moderate yields (Table 1, entry 16–19). Following known procedure for this kind of reactions,<sup>42,43</sup> the syntheses were performed in DMF in the presence of  $K_2CO_3$ , at 80 °C for 24 hours. In comparison to alcoxides in which the negative charge is located only on the oxygen atom, phenoxides are much softer nucleophiles therefore, the reactions proceeded efficiently.



This journal is © The Royal Society of Chemistry 2019

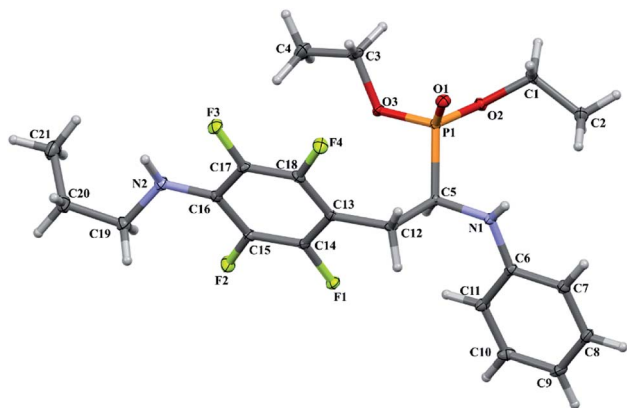


Fig. 2 A perspective view showing the asymmetric part of unit cell of 2I together with the labelling atoms scheme. Ellipsoids are drawn at the 30% probability level, hydrogen atoms are represented by spheres of arbitrary radii.

## 2.2 X-ray and DFT studies

In order to comprehensively understand the structural features of compounds investigated we made attempts to grow their crystals by slow evaporation of toluene solutions under ambient conditions. This process resulted in obtaining crystals suitable for X-ray single crystal diffraction analysis only for **2k** and **2l**. In terms of chemistry, compounds **2k** and **2l** differ in the chain length of substituent in *para* position of the fluorinated ring; **2k** contains the methylamine group, while propylamine group is present in **2l**. Molecules of **2k** and **2l** are chiral, however, they are not enantiomerically pure since the racemic mixture of substrate (**1a**) was used for their synthesis. Thus, crystallization yielded single crystals containing both enantiomers. Since the nitrogen atoms included in the molecular structure of **2k** and **2l** are pyramidal in shape, *i.e.* are bonded to three different groups and possess lone pair of electrons, they constitute stereogenic centres. This, in turn, may affect the occurrence of diastereomers in the crystals.

Both compounds examined crystallize in the triclinic space group *P*-1. **2k** crystallizes with two molecules (mol 1 and mol 2) in the asymmetric unit that adopt a similar molecular conformation described by two torsion angles Csp<sup>2</sup>-N-Csp<sup>3</sup>-Csp<sup>3</sup> and Csp<sup>2</sup>-Csp<sup>3</sup>-Csp<sup>3</sup>-N. The torsion angle values are -131.3(3)° and -83.9(3)° for mol 1, and 147.3(2)° and -68.9(3)° for mol 2, while

the dihedral angle of two aromatic rings are  $68.6(3)^\circ$  and  $78.0(3)^\circ$  in mol 1 and 2, respectively. Adoption of very similar conformation (marked as a conformation B), by some phosphonates analogues of fluorophenylalanine was previously observed in our research group.<sup>33</sup> The main structural differences are displayed within the aliphatic diethyl phosphonate chains ( $\text{Csp}^3\text{-Csp}^3\text{-O-P}$ ) where the chains adopt anti-periplanar-antiperiplanar conformation with the corresponding torsion angle values of  $-171(3)$  and  $165.7(2)^\circ$  for mol 1, while the synclinal-antiperiplanar conformation is characterized by the values of  $65.5(4)$  and  $176.1(2)^\circ$  for mol 2. Interestingly, the configuration of the aniline nitrogen atom in both symmetrically independent molecules shows the opposite stereochemistry *i.e.* *S* in mol 1 and *R* in mol 2; however, the methylamine moieties have the same *R* configuration. As a consequence these two molecules possess *R*(C5), *S*(N1), *R*(N2) and *R*(C24), *R*(N3), *R*(N4) configurations, respectively. Therefore they are diastereomers. Since the crystals of **2k** are centrosymmetric, two pairs of diastereomers coexist in the crystal structure. The pyramidal environment of N atom in methylamine group also affects significant deviation of this group from the tetrafluorophenyl plane; the  $\text{Csp}^2\text{-Csp}^2\text{-N-Csp}^3$  torsion angle is  $18.6(5)^\circ$  in mol 1 and  $21.2(4)^\circ$  in mol 2. In contrast, **2l** crystallizes with one molecule in the asymmetric unit and adopts previously described conformation C (extended)<sup>33</sup> with the corresponding torsion angles of  $80.3(2)^\circ$  and  $-172.4(2)^\circ$ . The anticlinal-antiperiplanar combination of the aliphatic diethyl phosphonate chains have torsion angles of  $107.5(2)$  and  $178.8(2)^\circ$ . The propylamine group adopts a folded conformation with an  $\text{N-Csp}^3\text{-Csp}^3\text{-Csp}^3$  torsion angle of  $62.5(3)^\circ$ . The stereochemistry of nitrogen atoms in this group is *S* while in the aniline moiety is *R*, hence the molecule in the asymmetric unit has a *R*(C5), *R*(N1), *S*(N2) configuration. The crystals investigated were chosen such that the *R* stereogenic centre at the carbon atom constitutes the asymmetric unit. The molecular structures of **2k** and **2l** are shown in Fig. 1 and 2.

The different configuration exhibited by the aniline nitrogen atoms in **2k**, prompted us to use quantum-chemical methods to study energy differences between the diastereomers. For this purpose all possible stereomers (*R,R,R*; *R,S,S*; *R,S,R*; *R,R,R*) were built based on the geometry of mol 1 derived from the crystal. The calculations were performed *in vacuo*, as well as using the polarisable continuum model (PCM) to take into account the

**Table 2** Relative energies ( $\Delta E$  (kcal mol<sup>-1</sup>))<sup>a</sup>, zero-point energy (ZPE (kcal mol<sup>-1</sup>))<sup>b</sup>, thermal correction to Gibbs free energy (TCG (kcal mol<sup>-1</sup>))<sup>c</sup> and percentage of populations (Pop) calculated for 2k stereomers *in vacuo* and using PCM for chloroform at the WB97XD/6-31+G(d) level of theory. Not that the absolute configuration *R* is imposed at the C5 and C24 carbon atoms

Stereomer	$\Delta E$ in <i>vacuo</i>	$\Delta E$ in chloroform	ZPE	TCG	Pop in <i>vacuo</i>	Pop in chloroform
<i>R,S,R</i>	0.00	5.12	0.00	0.00	98.9	<1.0
<i>R,S,S</i>	2.35	5.25	0.15	0.50	1.0	<1.0
<i>R,R,S</i>	5.77	1.88	0.39	0.97	<1.0	20.2
<i>R,R,R</i>	5.90	0.00	0.78	2.00	<1.0	79.1

<sup>a</sup> Relative energies calculated with respect to the lowest energy structure at WB97XD/6-31+G(d) level is equal to -1813.40587669 hartree. <sup>b</sup> Zero-point energy; the lowest value was equal to 0.412559 hartree. <sup>c</sup> Thermal correction to Gibbs free energy at 298 K; the lowest value was equal to 0.348198 hartree. The relative energy in chloroform was equal to -1813.41658767 hartree.

**Table 3** Valence angles values at nitrogen atoms in crystal structure of **2k** (X-ray), and calculated at the WB97XD/6-31+G(d) level of theory (DFT). The numbering of valence angles are the same as numbering atoms scheme in Fig. 1. Not that the absolute configuration *R* is imposed at the C5 and C24 carbon atoms

The valence angle [°]	Stereomer					
	<i>R,S,R</i> DFT	X-ray	<i>R,R,R</i> DFT	X-ray	<i>R,R,S</i> DFT	<i>R,S,S</i> DFT
C6–N1–H1 or C25–N3–H3	112.3	116.7	113.6	115.2	114.2	113.1
C5–N1–H1 or C24–N3–H3	113.2	115.8	112.3	117.1	113.1	113.3
C6–N1–C5 or C25–N3–C24	126.1	125.4	123.1	124.9	123.5	126.2
<b>Sum of the valence angles</b>	<b>351.6</b>	<b>357.9</b>	<b>349.0</b>	<b>357.2</b>	<b>350.8</b>	<b>352.6</b>
C16–N2–H2 or C35–N4–H4	111.6	115.9	111.1	113.9	111.5	111.5
C19–N2–H2 or C38–N4–H4	113.4	116.9	112.8	113.2	113.2	113.3
C16–N2–C19 or C35–N4–C38	121.8	125.2	120.7	123.3	121.6	121.5
<b>Sum of the valence angles</b>	<b>346.8</b>	<b>358.0</b>	<b>344.9</b>	<b>350.4</b>	<b>346.3</b>	<b>346.3</b>

effect of chloroform solution as NMR spectra of **2k** were recorded for the compound sample dissolved in CDCl<sub>3</sub>.

The results obtained support structural diversity of the possible stereomers. The results show that the *R,R,R* stereomer is energetically favourable at WB97XD/6-31+G(d) level of theory including PCM, while *in vacuo* the lowest relative energy is assigned to the *R,S,R* stereomer (Table 2).

These findings suggest a strong influence of surrounding medium on the energy preferences of stereomers (diastereomers). *In vacuo* the *R,S,R* stereomer constitutes over 98% in the

population of the calculated diastereomers (Table 2). Its population drops below 1% when chloroform solvent is taken into consideration *via* PCM approximation. In chloroform *R,R,R* stereomer seems to be predominant as it constitutes almost 80% in the population of diastereomers – a striking difference with its contribution (below 1%) *in vacuo*.

Analysis of the nitrogen atoms pyramidal environment in both the optimized and crystal structures of **2k** shows strong deviation from the ideal tetrahedral geometry, described by set of valence angles equal to 109.5°, towards the planar one. As

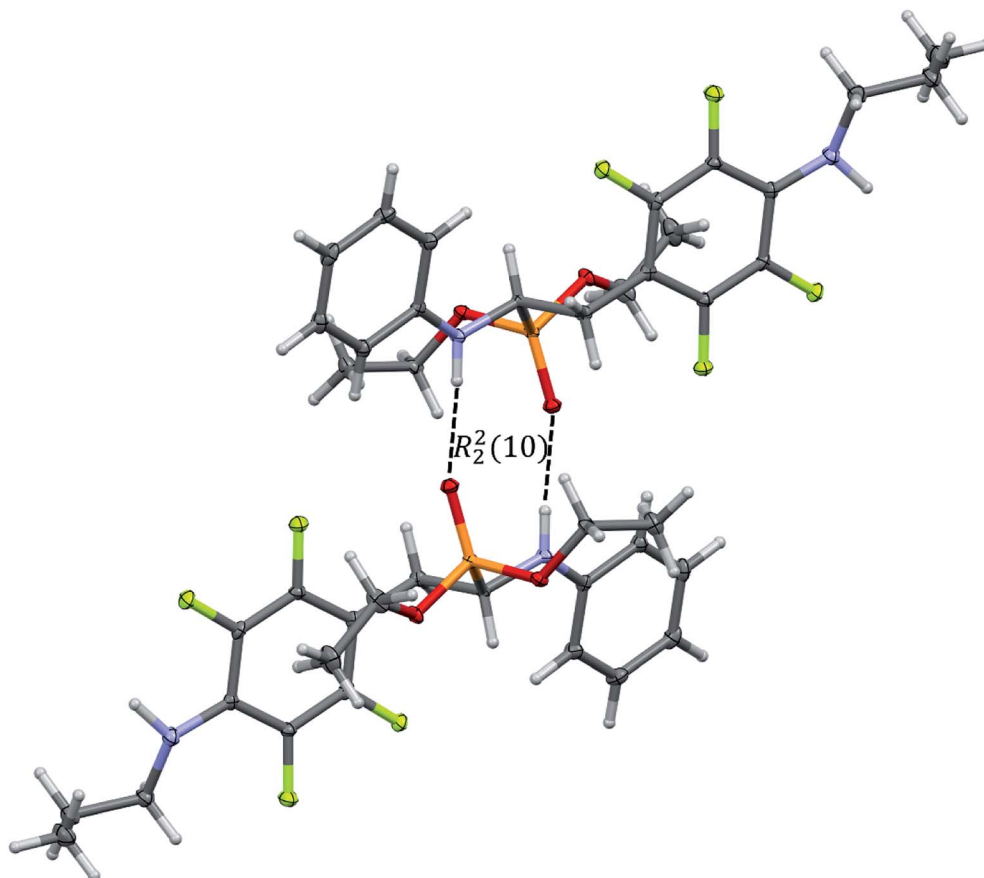


**Fig. 3** Dimeric motif of N–H···O(=P) hydrogen bonds between two enantiomers of opposite stereochemistry in the crystals of **2l**. This motif is also observed in the crystals of **2k**.

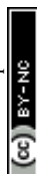




Table 4 Geometrical parameters describing the N–H...O interactions in the crystals of **2k** and **2l**

	D–H [Å]	H...A [Å]	D...A [Å]	D–H...A [°]	SYMM
<b>2k</b>					
N1–H1...O1	0.81(2)	2.16(2)	2.975(3)	177(2)	$[-x + 2, -y + 1, -z + 1]$
N3–H3...O4	0.86(2)	2.12(3)	2.964(2)	168(3)	$[-x + 1, -y + 1, -z]$
<b>2l</b>					
N1–H1...O1	0.85(3)	2.03(3)	2.871(3)	173(2)	$[-x + 1, -y + 2, -z + 1]$

seen in Table 3, the valence angles values in both structures are similar. For example, in the crystal structure the values of C6–N1–H1, C5–N1–H1 and C6–N1–C5 valence angles are equal to 116.7°, 115.8°, and 125.4°, in mol 1, and 115.2°, 117.1°, and 124.9° for C25–N3–H3, C24–N3–H3 and C24–N3–C25 in mol 2, while in the calculated *R,R,R* stereomer the corresponding valence angles adopt values of 113.6°, 112.3° and 123.1° (Table 3). The sum of the valence angles values in the crystal structure is equal to 357.9° and 357.2°, in mol 1 and mol 2, respectively, and 349° in the *R,R,R* stereomer calculated. All these values correspond to forms between the ideally planar (360°) and ideally tetrahedral (328.5°) geometry but closer to the planar one.

The bond order analysis showed that bond order for the bond between C6–N1 (nitrogen atom attached to the carbon atom in the phenyl ring) is *ca* 1.10. For the bond between C16–N2 (nitrogen atom attached to the carbon atom in the

perfluorinated phenyl ring) the bond order is *ca* 1.12, further explaining partially planar arrangement at the nitrogen atoms. Indeed the pyramidal shape at the N atom can invert its configuration in the structures investigated. The energy barrier of transition between the diastereomers (invertomers) was estimated in DFT calculations to *ca* 2.7 kcal mol<sup>−1</sup> *in vacuo*. The temperature of coalescence (*T<sub>c</sub>*) was approximated to *ca* 53 K in accordance to eqn (2) (Experimental section). The transition energy in chloroform differed from the value calculated *in vacuo* conditions, and was estimated to *ca* 2.5 kcal mol<sup>−1</sup>. The *T<sub>c</sub>* temperature was approximated to *ca* 50 K.

Our quantum chemical computational results refer to isolated molecule or a molecule in a polarisable continuum that model chloroform solution. On the other hand in the solid state the molecules can interact with the actual molecules in the crystal environment. Unfortunately, the attempt to perform calculations with PBC (Periodic Boundary Conditions) for such

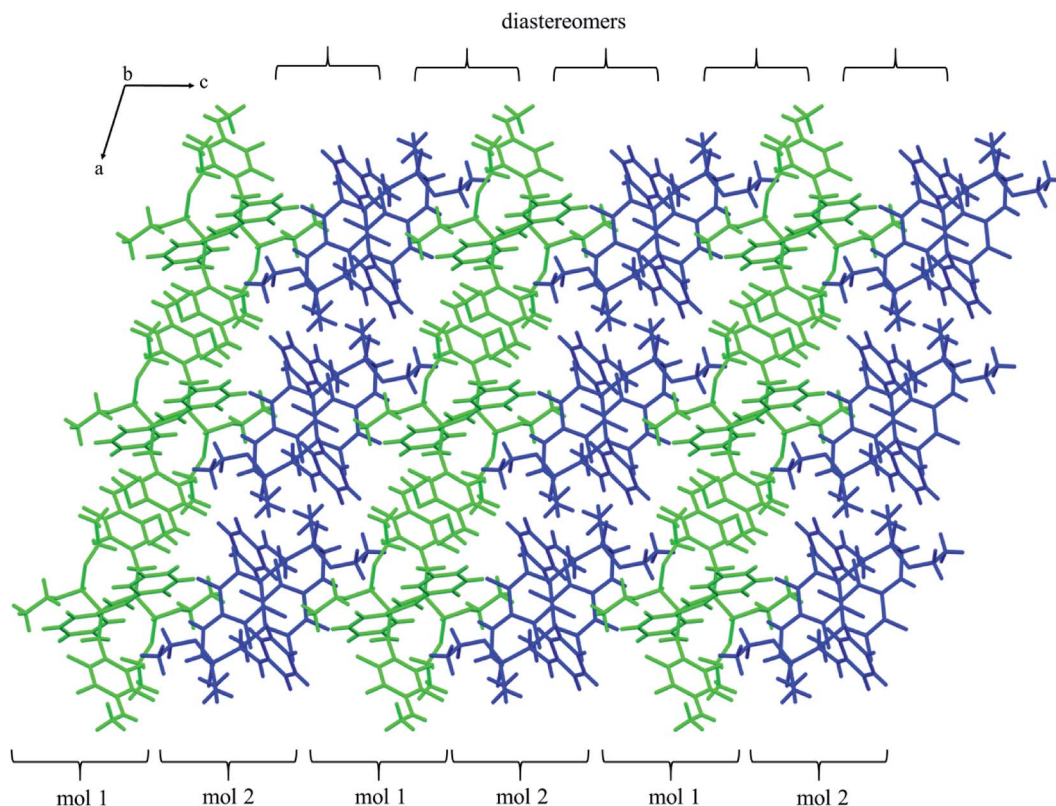


Fig. 4 Self-sorting of diastereomers on supramolecular level in the crystals of **2k**. Two symmetry independent molecules that represent two diastereomers (mol 1 and mol 2) were distinguished by green and blue colors.



**Table 5** Geometrical parameters for other types of intermolecular interactions that occurs in the crystals investigated

	D–H [Å]	H⋯A [Å]	D⋯A [Å]	D–H⋯A [°]	SYMM
<b>2k</b>					
C11–H11⋯F7	0.95	2.55(3)	3.333(4)	140(3)	$[x + 1, y, z]$
C22–H22A⋯F3	0.99	2.55(3)	3.387(4)	143(3)	$[-x + 1, -y + 1, -z]$
C26–H26⋯F3	0.95	2.42(2)	3.153(3)	134(3)	
N4–H4⋯O1	0.85(3)	2.29(4)	3.074(3)	154(3)	$[-x + 1, -y + 1, -z + 1]$
N2–H2⋯F7	0.79(3)	2.53(3)	3.017(3)	121(3)	
C22–H22A⋯ $\pi$	0.99	2.78(4)	3.486(5)	129(4)	$[-x + 1, -y + 1, -z]$
C22–H22B⋯ $\pi$	0.99	2.67(5)	3.529(6)	145(5)	$[-x + 1, -y + 1, -z]$
C28–H28⋯F5	0.95	2.67(3)	3.299(3)	125(3)	$[-x, -y, -z]$
<b>2l</b>					
C1–H1B⋯F1	0.99	2.59(3)	3.339(2)	133(2)	$[-x + 2, -y + 2, -z + 1]$
C5–H5⋯O2	1.00	2.62(2)	3.526(2)	152(2)	$[-x + 2, -y + 2, -z + 1]$
N2–H2⋯F3	0.98(3)	2.19(3)	3.159(2)	171(2)	$[-x + 1, -y + 1, -z]$

enantiomers of opposite stereochemistry together around a centre of symmetry, as shown in Fig. 3. Geometrical parameters describing hydrogen bonds are listed in Table 4. It is worth

In the crystal structures of **2k** and **2l** the principal interactions are N-H $\cdots$ O(=P) hydrogen bonds that hold two

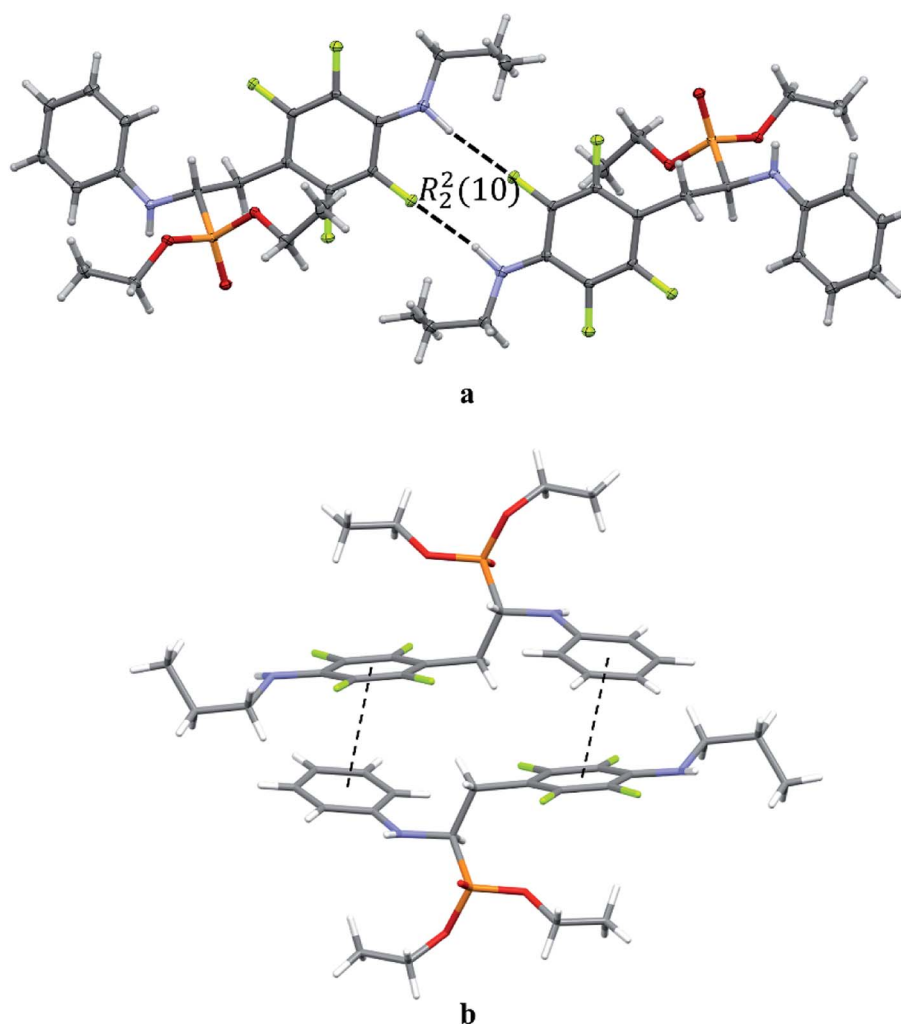


Fig. 5 Dimeric motif of N—H...F interactions (a) and  $\pi\cdots\pi$  interactions between two enantiomers of opposite stereochemistry in the crystals of **2l** (b).



noting that in **2k** this motif occurs between enantiomers but not between diastereomers.

The self-sorting phenomenon of diastereomers at supramolecular level is observed in the crystals of **2k**. Since there are two diastereomers in the asymmetric unit, each of them forms separate layer perpendicular to *c* lattice direction containing pairs of enantiomers. The layers are stabilized by the previously mentioned N–H...O(=P) hydrogen bonds, which are supported by interactions involving  $\pi$ -electrons. The fluorinated rings of two neighbouring mol 1 oriented parallel to each other favours the formation of  $\pi$ ... $\pi$  interactions between these moieties, while a tilted arrangement of fluorinated and non-fluorinated aromatic rings of two mol 2 leads to formation of H... $\pi$  and H...F contacts (2.77(3) and 2.67(3) Å, respectively) that are equal or shorter than the sum of van der Waals radii of hydrogen and carbon atoms ( $H_{vdW} = 1.2$  Å,  $C_{vdW} = 1.7$  Å, the sum = 2.9 Å),<sup>45</sup> and hydrogen and fluorine atoms ( $F_{vdW} = 1.47$  Å, the sum is 2.67 Å).<sup>45</sup> The geometrical parameters describing  $\pi$ ... $\pi$  interactions are 3.319(3) and 0.88 Å for distance between the planes of aromatic rings along with the offset, respectively. The two layer types are alternately arranged in the crystal as shown in Fig. 4, and are related to each other through N–H...O(=P) hydrogen bonds in which the methylamine group acts as a donor of hydrogen bonds. The geometrical parameters of the hydrogen bond listed in Table 5 suggest that the interactions between diastereomers are slightly weaker than those between enantiomers in the layer. Moreover, the proximity of the aromatic rings and ester group belonging to diastereomers in two neighbouring layers promotes the formation of multiple H...F and H...F interactions and thus substantially affects the crystal structure stabilization.

The extended C molecular conformation of **2l** favours self-association forming dimers in which the two molecules interact *via* N–H...F hydrogen bonding and strong affects the formation of isolated  $\pi$ ... $\pi$  intermolecular interactions between fluorinated and non-fluorinated aromatic rings as shown in Fig. 5. The interacting rings are tilted toward each other by 16° while the interplanar distance between the centres of gravity is

3.796 Å. The intermolecular interactions present in the crystals are reported in Table 5.

### 2.3 Biological evaluation

Six randomly chosen  $S_NAr$  reactions products, and also six of the fluorinated phosphonate analogues of phenylalanine, including **1a**, previously synthesized in our research group,<sup>33</sup> were subjected to biological studies. The first group of compounds contained mainly different thiophenols derivatives, while various  $\alpha$ -aminophosphonates differing in number and position of fluorine substituents in one of the phenyl rings constituted the second group.

In the compounds molecules, apart from amino group, two additional pharmacophores are present; fluorine substituents and phosphonate group that replaced an amino acid carbonyl one. A considerable number of  $\alpha$ -aminophosphonates is known to exhibit various biological activities including anticancer one. On the other hand, a lot of existing drugs, for example synthetic statins and 5-fluorouracil, contain fluorine. This shows a remarkable potential of fluorine in pharmaceutical chemistry and provide a source for drug discovery.<sup>18</sup> Therefore combination of fluorine pharmacophore with amino and phosphonate group in molecules of target compounds was expected to have an impact on their bioactivity.

**2.3.1 Drug likeness.** With the aim to develop novel anti-proliferative therapeutics, which are orally bioavailable and focusing particularly on glioma treatment, human intestinal absorption and blood–brain barrier penetration of  $\alpha$ -aminophosphonates were calculated. The structure-based prediction models depended on physicochemical and molecular properties of the compounds were performed with various computing software.

The most common criteria used for preliminary evaluation of drug likeness of a compound encompass the Lipinski's "rule of 5".<sup>46,47</sup> In this respect, the physicochemical parameters of the examined compounds generally match the rule (Table 6).

According to Veber's rule, reduced molecular flexibility, as measured by the number of rotatable bonds, and low polar surface area or total hydrogen bond count (sum of donors and

Table 6 Selected physicochemical data for the studies  $\alpha$ -aminophosphonates<sup>a</sup>

Cpd	MW	aPSA [Å <sup>2</sup> ]	PSA [Å <sup>2</sup> ]	log <i>P</i>	HBD	HBA	RB	Caco-2 [nm s <sup>-1</sup> ]	BB	MDCK [nm s <sup>-1</sup> ]
<b>1a</b>	423.31	303.9	8.7	4.22	1	4	9	21.72	1.38	86.84
<b>1b</b>	385.80	294.6	13.5	4.27	1	4	9	21.79	1.30	102.26
<b>1c</b>	385.80	312.7	8.7	4.25	1	4	9	21.74	1.27	104.23
<b>1d</b>	383.37	295.7	13.5	4.18	1	4	9	21.72	1.26	116.53
<b>1e</b>	351.35	297.4	8.7	3.64	1	4	9	21.72	0.98	168.46
<b>1f</b>	387.34	283.1	13.5	3.95	1	4	9	21.72	1.00	109.96
<b>2b</b>	527.52	364.9	27	6.25	1	4	11	21.72	1.06	42.40
<b>2d</b>	543.52	363.8	35.3	5.75	1	5	12	21.72	0.18	12.35
<b>2e</b>	543.52	367.5	36	5.75	1	5	12	21.72	0.18	14.77
<b>2f</b>	528.51	325.4	52	5.18	3	5	11	21.70	0.19	3.94
<b>2j</b>	580.15	329.0	81.8	3.75	2	8	15	21.69	0.01	0.06
<b>2r</b>	531.87	361.8	13.4	5.92	1	5	11	21.73	3.06	44.20

<sup>a</sup> MW – molecular weight, aPSA – apolar surface area, PSA – polar surface area, log *P* – an octanol–water partition coefficient calculated with ALOGPS 2.1, HBD – number of hydrogen bond donors, HBA – number of hydrogen bond acceptors, RB – rotatable bonds number.





Table 7 Cytotoxicity (IC<sub>50</sub>) values of the studies  $\alpha$ -aminophosphonates

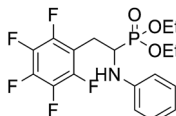
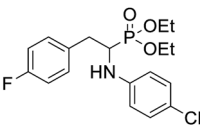
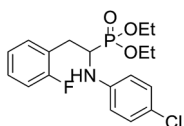
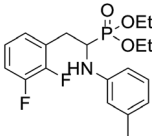
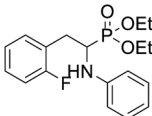
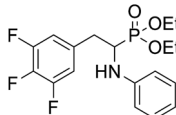
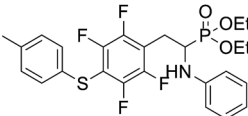
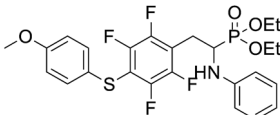
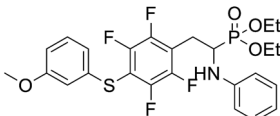
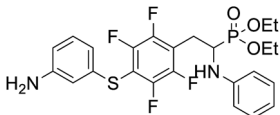
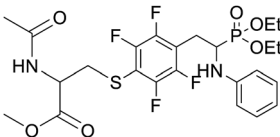
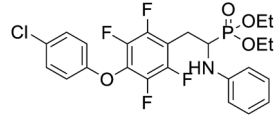
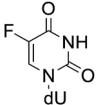
Compound	Compound structure	T98G IC <sub>50</sub> [ $\mu$ M]	U-118 MG IC <sub>50</sub> [ $\mu$ M]	HaCaT IC <sub>50</sub> [ $\mu$ M]
1a		40.4 $\pm$ 6.2	60.67 $\pm$ 8.9	56.8 $\pm$ 7.4
1b		73.5 $\pm$ 9.2	88.2 $\pm$ 7.5	>100
1c		67.9 $\pm$ 11.2	91.2 $\pm$ 15.5	>100
1d		71.3 $\pm$ 8.7	48.6 $\pm$ 10.4	67.9 $\pm$ 11.8
1e		106.4 $\pm$ 14.7	86.8 $\pm$ 7.2	61.8 $\pm$ 9.1
1f		25.1 $\pm$ 4.5	40.8 $\pm$ 8.4	33.2 $\pm$ 5.1
2b		14.5 $\pm$ 3.3	37.9 $\pm$ 2.5	26.5 $\pm$ 4.7
2d		36.8 $\pm$ 5.7	33.2 $\pm$ 7.3	19.8 $\pm$ 3.9
2e		20.4 $\pm$ 3.1	21.4 $\pm$ 2.7	10.1 $\pm$ 2.2
2f		25.5 $\pm$ 1.9	28.1 $\pm$ 3.6	18.2 $\pm$ 3.4
2j		82.7 $\pm$ 15.7	>100	>100
2r		70.3 $\pm$ 8.3	79.2 $\pm$ 6.4	48.4 $\pm$ 7.4



Table 7 (Contd.)

Compound	Compound structure	T98G IC <sub>50</sub> [μM]	U-118 MG IC <sub>50</sub> [μM]	HaCaT IC <sub>50</sub> [μM]
5-FdU (5-fluoro-2'-deoxyuridine)		5.57 ± 0.9	23.40 ± 1.6	4.42 ± 1.1

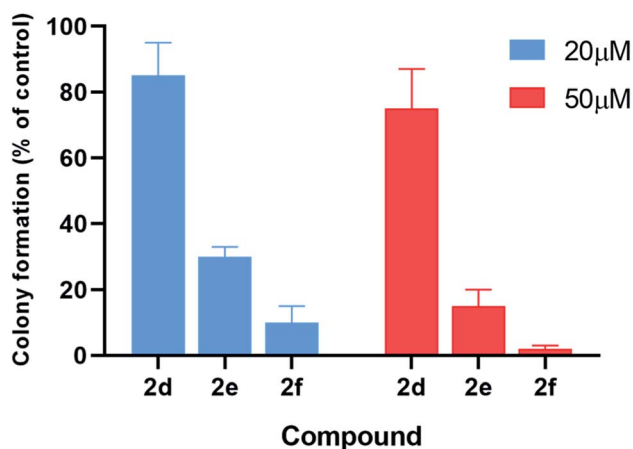


Fig. 6 Treatment with compounds **2d–f** significantly reduces the colony-forming ability of T98G cells as compared to untreated cells. Error bars display the standard deviation from at least three independent measurements.

acceptors) are found to be important predictors of good oral bioavailability, independent of molecular weight.<sup>48</sup> Veber's observations suggest that compounds which meet only the two criteria: 10 or fewer rotatable bonds and polar surface area equal to or less than 140 Å<sup>2</sup> (or 12 or fewer H-bond donors and acceptors) will have a high probability of good oral bioavailability. All of the examined compounds meet these criteria perfectly (Table 6).

Caco-2 cell permeability model classifies compounds into 3 classes of permeability (high, medium and low). Compounds with  $t_{\text{Papp}}$  below 4 nm s<sup>-1</sup> are classified as low permeable; compounds with  $t_{\text{Papp}}$  above 70 nm s<sup>-1</sup> are classified as high permeable and compounds with permeability values between 4–70 nm s<sup>-1</sup> are classified as medium.<sup>49</sup> For blood–brain barrier penetration we calculated the BB value which is defined as the ratio of the concentration of a drug in the brain and in the blood, measured at equilibrium ( $\text{BB} = C_{\text{Brain}}/C_{\text{Blood}}$ ). Compounds with  $\text{BB} > 2.0$  cross the blood–brain barrier readily (high absorption to CNS (central nervous system)) while molecules with  $\text{BB} < 0.1$  are poorly distributed to the brain (low absorption to CNS).<sup>50</sup> Results show that all compounds are characterized by a good intestinal absorption (20–80%) and relatively high brain penetration, therefore making these compounds more druggable (Table 6).

**2.3.2 In vitro cytostatic activity.** Two glioblastoma multi-forme cell lines: T98G and U118 MG, and HaCaT as referential

healthy cells were chosen. For comparison, IC<sub>50</sub> values reflecting inhibitory activity of known anticancer drug 5-fluoro-2'-deoxyuridine in the chosen cell lines were included in Table 7.

As shown in this table, all compounds exhibited moderate cytostatic activity in the both glioblastoma cell lines. Most of the compounds showed higher activity against T98G cell line. Only **1d**, **1e** and to a small degree also **2d** occurred to be better inhibitors of U-118MG cell line. Most of the studied S<sub>N</sub>Ar reactions products displayed significantly higher inhibitory activity against both glioblastoma multi-forme cell lines than the parent α-aminophosphonate **1a**. This indicates that the introduction of thiophenols, but not aliphatic thiols nor phenols, to the *para* position in the fluorinated phenyl ring of **1a** molecule improve the anti-glioma activity. IC<sub>50</sub> values also demonstrate that for compounds **2b**, **2d**, **2e** and **2f**, the substituents in the thiophenol moiety had an influence on the cytotoxic activity (Table 7). All these substituents belong to EDG and it can be concluded that less electrodonating character of CH<sub>3</sub> group than of OCH<sub>3</sub> and NH<sub>2</sub> groups, results in higher activity of **2b** in comparison with **2d–2f**. Among the S<sub>N</sub>Ar reactions products studied, **2b** exhibiting the highest cytotoxic activity against T98G cell line and good selectivity can be considered as the best candidate for anti-glioma drug.

Analysis of IC<sub>50</sub> values for α-aminophosphonates **1a–1f**, indicates that number of fluorine substituents in one aromatic ring as well as presence and character of substituents in the second ring contribute to the anticancer activity displayed by these compounds. Compounds **1b** and **1c** containing one fluorine and one chlorine atoms, exhibit very similar inhibitory activity against both cancer cell lines indicating that position of this fluorine atom does not influence much the activity. Comparing these compounds with the **1e** demonstrates that chlorine substituent may constitute an important factor contributing to anticancer activity. Number of fluorine substituents also seems to have impact on the cytotoxic inhibition, though the influence is irregular.

The inhibitory effects of α-aminophosphonates in T98G cells were further assessed by performing clonogenic assays (Fig. 6). Compounds **2d–f** were also significantly more potent than other compounds in this assay. Treatment with 20 μM **2d–f** resulted in clonogenic survival of 85%, 30%, and 10%, respectively, compared to control cells. When we tested the effect of each compound at 50 μM, we found that **2d** reduces cancer cell clonogenic potential by 25%, **2e** by 85%, and **2f** by 98%.



## RSC Adv., 2019, 9, 24117–24133 | 24127

7.05–7.01 (m, 2H, 2CHar), 6.91–6.89 (m, 3H, 3 CHar), 6.72 (d,  $J$  = 7.8 Hz, 2H, 2CHar), 6.57 (t,  $J$  = 7.3 Hz, 1H, CHar), 4.89–4.86 (m, 1H, NH), 4.13–4.02 (m, 5H, CH, 2OCH<sub>2</sub>), 3.33–3.30 (m, 1H, ArCH<sub>2</sub>), 3.23–3.13 (m, 1H, ArCH<sub>2</sub>), 2.83 (s, 6H, 2 ArCH<sub>3</sub>), 1.23 (t,  $J$  = 7.1 Hz, 3H, CH<sub>3</sub>), 1.17 (t,  $J$  = 7.1 Hz, 3H, CH<sub>3</sub>). <sup>19</sup>F NMR (377 MHz, CDCl<sub>3</sub>)  $\delta$  = –133.72 to –133.81 (m, 2F), –142.38 (dd,  $J$  = 24.4, 11.9 Hz, 2F). <sup>31</sup>P NMR (162 MHz, acetone-*d*<sub>6</sub>)  $\delta$  = 23.10 (s). <sup>13</sup>C NMR (101 MHz, CDCl<sub>3</sub>)  $\delta$  = 148.13–145.45 (m, 2Car), 146.78–144.11 (m, 2Car) 146.30 (d,  $J$  = 6.5 Hz, Car), 139.06 (s, Car), 132.63 (s, 2Car), 129.69 (s, CHar) 129.31 (s, 2CHar), 128.05 (s, 2CHar), 118.87 (s, CHar), 118.13–117.64 (m, Car), 113.49 (s, 2CHar), 112.67–112.26 (m, Car), 63.69 (d,  $J$  = 7.0 Hz, OCH<sub>2</sub>), 62.44 (d,  $J$  = 7.4 Hz, OCH<sub>2</sub>), 50.60 (d,  $J$  = 157.4 Hz, CH), 25.09 (d,  $J$  = 7.3 Hz, ArCH<sub>2</sub>), 21.28 (s, 2 ArCH<sub>3</sub>), 16.56, 16.51, 16.44, and 16.38 (2CH<sub>3</sub>). HRMS (ESI<sup>+</sup>) calcd for C<sub>26</sub>H<sub>29</sub>F<sub>4</sub>NO<sub>3</sub>PS (M + H)<sup>+</sup>: 542.1542, found: 542.1542.

**4.1.2.4 Diethyl (1-(phenylamino)-2-(2,3,5,6-tetrafluoro-4-((methoxyphenyl)thio)phenyl)ethyl)phosphonate (2d).** Pale yellow solid (61 mg, 95%), mp = 93–95 °C. <sup>1</sup>H NMR (400 MHz, acetone-*d*<sub>6</sub>)  $\delta$  = 7.30–7.28 (m, 2H, 2CHar), 7.05–6.98 (m, 2H, 2CHar), 6.92–6.90 (m, 2H, 2CHar), 6.68 (d,  $J$  = 7.8 Hz, 2H, 2CHar), 6.58 (t,  $J$  = 7.2 Hz, 1H, CHar), 4.85–4.82 (m, 1H, NH), 4.11–4.06 (m, 5H, CH, 2OCH<sub>2</sub>), 3.80 (s, 3H, ArCH<sub>3</sub>), 3.31–3.27 (m, 1H, ArCH<sub>2</sub>), 3.19–3.10 (m, 1H, ArCH<sub>2</sub>), 1.23 (t,  $J$  = 7.1 Hz, 3H, CH<sub>3</sub>), 1.17 (t,  $J$  = 7.1 Hz, 3H, CH<sub>3</sub>). <sup>19</sup>F NMR (377 MHz, CDCl<sub>3</sub>)  $\delta$  = –134.67 (dd,  $J$  = 24.0, 11.8 Hz, 2F), –142.70 (dd,  $J$  = 24.3, 12.2 Hz, 2F). <sup>31</sup>P NMR (162 MHz, acetone-*d*<sub>6</sub>)  $\delta$  = 23.04 (s). <sup>13</sup>C NMR (101 MHz, CDCl<sub>3</sub>):  $\delta$  = 159.95 (s, Car), 147.79–145.13 (m, 2Car), 146.70–144.00 (m, 2Car), 146.30 (d,  $J$  = 7.1 Hz, Car), 134.07 (s, 2CHar), 129.25 (s, 2CHar), 123.25 (s, Car), 118.74 (s, CHar), 117.61–117.11 (m, Car), 114.88 (s, 2CHar), 114.14–113.69 (m, Car), 113.36 (s, 2CHar), 63.69 (d,  $J$  = 7.0 Hz, OCH<sub>2</sub>), 62.43 (d,  $J$  = 7.4 Hz, OCH<sub>2</sub>), 55.44 (s, OCH<sub>3</sub>), 50.47 (d,  $J$  = 158.1 Hz, CH), 25.00 (s, ArCH<sub>2</sub>), 16.54, 16.49, 16.42, 16.36 (2CH<sub>3</sub>). HRMS (ESI<sup>+</sup>) calcd for C<sub>25</sub>H<sub>27</sub>F<sub>4</sub>NO<sub>4</sub>PS (M + H)<sup>+</sup>: 544.1335, found: 544.1339.

**4.1.2.5 Diethyl (1-(phenylamino)-2-(2,3,5,6-tetrafluoro-4-((3-methoxyphenyl)thio)phenyl)ethyl)phosphonate (2e).** Yellow oil (61 mg, 95%). <sup>1</sup>H NMR (400 MHz, acetone-*d*<sub>6</sub>)  $\delta$  = 7.23 (t,  $J$  = 8.0 Hz, 1H, CHar), 7.06–7.02 (m, 2H, 2CHar), 6.85–6.80 (m, 2H, 2CHar), 6.71 (d,  $J$  = 7.9 Hz, 1H, 2CHar), 6.66 (d,  $J$  = 7.9 Hz, 1H, CHar), 6.59 (t,  $J$  = 7.3 Hz, 1H, CHar), 4.88–4.86 (m, NH), 4.15–4.04 (m, 5H, 2OCH<sub>2</sub>, CH), 3.75 (s, 3H, OCH<sub>3</sub>), 3.36–3.30 (m, 1H, ArCH<sub>2</sub>), 3.24–3.14 (m, 1H, ArCH<sub>2</sub>), 1.25 (t,  $J$  = 7.1 Hz, 3H, CH<sub>3</sub>), 1.19 (t,  $J$  = 7.0 Hz, 3H, CH<sub>3</sub>). <sup>19</sup>F NMR (377 MHz, CDCl<sub>3</sub>):  $\delta$  = –133.45 to –133.55 (m, 2F), –142.22 (dd,  $J$  = 24.4, 12.4 Hz, 2F). <sup>31</sup>P NMR (162 MHz, acetone-*d*<sub>6</sub>):  $\delta$  = 23.04 (s). <sup>13</sup>C NMR (101 MHz, CDCl<sub>3</sub>):  $\delta$  = 159.99 (s, Car), 148.10–145.44 (m, 2Car), 147.90–144.05 (m, 2Car), 146.28 (d,  $J$  = 6.9 Hz, Car), 134.52 (s, Car), 130.15 (s, CHar), 129.28–129.24 (s, 2CHar), 121.84 (s, CHar), 118.81 (s, CHar), 118.40–118.04 (m, Car), 115.25 (s, CHar), 113.34 (s, 2CHar), 113.12 (s, CHar), 111.88–111.47 (m, Car), 63.68 (d,  $J$  = 7.0 Hz, OCH<sub>2</sub>), 62.45 (d,  $J$  = 7.4 Hz, OCH<sub>2</sub>), 55.34 (s, OCH<sub>3</sub>), 50.48 (d,  $J$  = 157.9 Hz, CH), 25.12 (d,  $J$  = 7.3 Hz, ArCH<sub>2</sub>), 16.53, 16.47, 16.42, and 16.36 (2CH<sub>3</sub>). HRMS (ESI<sup>+</sup>) calcd for C<sub>25</sub>H<sub>27</sub>F<sub>4</sub>NO<sub>4</sub>PS (M + H)<sup>+</sup>: 544.1335, found: 544.1328.

**4.1.2.6 Diethyl (2-(4-((3-aminophenyl)thio)-2,3,5,6-tetrafluorophenyl)-1-(phenylamino)ethyl)phosphonate (2f).** Pale

yellow oil (47 mg, 76%). <sup>1</sup>H NMR (400 MHz, acetone-*d*<sub>6</sub>)  $\delta$  = 7.06–6.96 (m, 3H, 3 CHar), 6.71 (d,  $J$  = 8.3 Hz, 2H, 2CHar), 6.57 (m, 3H, 3 CHar), 6.35 (d,  $J$  = 8.2 Hz, 1H, CHar), 4.86–4.83 (m, 1H, NH<sub>2</sub>), 4.76–4.74 (m, 1H, NH<sub>2</sub>), 4.13–4.06 (m, 6H, CH, NH<sub>2</sub>OCH<sub>2</sub>), 3.35–3.29 (m, 1H, ArCH<sub>2</sub>), 3.23–3.14 (m, 1H, ArCH<sub>2</sub>), 1.24 (t,  $J$  = 7.1 Hz, 3H, CH<sub>3</sub>), 1.19 (t,  $J$  = 7.1 Hz, 3H, CH<sub>3</sub>). <sup>19</sup>F NMR (377 MHz, CDCl<sub>3</sub>)  $\delta$  = –133.46 (dd,  $J$  = 23.5, 11.4 Hz, 2F), –142.32 to –142.42 (m, 2F). <sup>31</sup>P NMR (162 MHz, acetone-*d*<sub>6</sub>)  $\delta$  = 23.04 (s). <sup>13</sup>C NMR (101 MHz, CDCl<sub>3</sub>)  $\delta$  = 148.19–145.53 (m, 2Car), 147.21 (s, Car), 146.65–144.08 (m, 2Car), 146.35 (d,  $J$  = 6.6 Hz, Car), 134.31 (s, Car), 130.12 (s, CHar), 129.35 (s, 2CHar), 119.61 (s, CHar), 118.80 (s, CHar), 118.37–117.88 (m, Car), 115.64 (s, CHar), 114.24 (s, CHar), 113.41 (s, 2CHar), 112.18–111.78 (m, Car), 63.68 (d,  $J$  = 7.0 Hz, OCH<sub>2</sub>), 62.51 (d,  $J$  = 7.4 Hz, OCH<sub>2</sub>), 50.56 (d,  $J$  = 157.9 Hz, CH), 25.09 (s, ArCH<sub>2</sub>), 16.58, 16.52, 16.47, and 16.42 (2CH<sub>3</sub>). HRMS (ESI<sup>+</sup>) calcd for C<sub>24</sub>H<sub>26</sub>F<sub>4</sub>N<sub>2</sub>O<sub>3</sub>PS (M + H)<sup>+</sup>: 529.1338, found: 529.1335.

**4.1.2.7 Diethyl (2-(4-((4-bromophenyl)thio)-2,3,5,6-tetrafluorophenyl)-1-(phenylamino)ethyl)phosphonate (2g).** Pale yellow solid (60 mg, 86%), mp = 77–79 °C. <sup>1</sup>H NMR (400 MHz, acetone-*d*<sub>6</sub>)  $\delta$  = 7.52–7.49 (m, 2H, 2CHar), 7.14–7.04 (m, 2H, 2CHar), 7.05–7.04 (m, 2H, 2CHar), 6.70 (d,  $J$  = 8.6 Hz, 2H, 2CHar), 6.61 (t,  $J$  = 7.4 Hz, 1H, CHar), 4.87–4.83 (m, 1H, NH), 4.16–4.05 (m, 5H, CH, 2OCH<sub>2</sub>), 3.36–3.29 (m, 1H, ArCH<sub>2</sub>), 3.24–3.18 (m, 1H, ArCH<sub>2</sub>), 1.26 (t,  $J$  = 7.1 Hz, 3H, CH<sub>3</sub>), 1.20 (t,  $J$  = 7.0 Hz, 3H, CH<sub>3</sub>). <sup>19</sup>F NMR (377 MHz, acetone-*d*<sub>6</sub>)  $\delta$  = –135.90 to –136.00 (m, 2F), –142.59 to –142.69 (m, 2F). <sup>31</sup>P NMR (162 MHz, acetone-*d*<sub>6</sub>)  $\delta$  = 22.89 (s). <sup>13</sup>C NMR (101 MHz, CDCl<sub>3</sub>)  $\delta$  = 148.05–145.38 (m, 2Car), 146.87–144.21 (m, 2Car) 146.33 (d,  $J$  = 7.2 Hz, Car), 132.59 (s, Car), 132.46 (s, 2CHar), 131.50 (s, 2CHar), 129.34 (s, 2CHar), 121.74 (s, Car), 118.79 (s, CHar), 118.49 (s, Car), 113.27 (s, 2CHar), 111.45 (s, Car), 63.78 (d,  $J$  = 7.0 Hz, OCH<sub>2</sub>), 62.54 (d,  $J$  = 7.4 Hz, OCH<sub>2</sub>), 50.43 (d,  $J$  = 158.6 Hz, CH), 25.23 (d,  $J$  = 7.5 Hz, ArCH<sub>2</sub>), 16.61, 16.56, 16.51, and 16.45 (2CH<sub>3</sub>). HRMS (ESI<sup>+</sup>) calcd for C<sub>24</sub>H<sub>24</sub>BrF<sub>4</sub>NO<sub>3</sub>PS (M + H)<sup>+</sup>: 592.0334, found: 592.0336.

**4.1.2.8 Diethyl (2-(4-((benzylthio)-2,3,5,6-tetrafluorophenyl)-1-(phenylamino)ethyl)phosphonate (2h).** Yellow oil (40 mg, 65%). <sup>1</sup>H NMR (400 MHz, acetone-*d*<sub>6</sub>)  $\delta$  = 7.33–7.20 (m, 1H, CHar), 7.17 (s, 4H, 4 CHar), 7.08–7.04 (m, 2H, 2CHar), 6.70 (d,  $J$  = 7.9 Hz, 2H, 2CHar), 6.59 (t,  $J$  = 7.3 Hz, 1H, CHar), 4.82–4.79 (m, 1H, NH), 4.13–4.02 (m, 7H, SCH<sub>2</sub>, CH, 2OCH<sub>2</sub>), 3.30–3.24 (m, 1H, ArCH<sub>2</sub>), 3.17–3.08 (m, 1H, ArCH<sub>2</sub>), 1.24 (t,  $J$  = 7.1 Hz, 3H, CH<sub>3</sub>), 1.17 (t,  $J$  = 7.1 Hz, 3H, CH<sub>3</sub>). <sup>19</sup>F NMR (377 MHz, acetone-*d*<sub>6</sub>)  $\delta$  = –136.30 to –136.40 (m, 2F), –143.81 to –143.90 (m, 2F). <sup>31</sup>P NMR (162 MHz, acetone-*d*<sub>6</sub>)  $\delta$  = 23.13 (s). <sup>13</sup>C NMR (101 MHz, CDCl<sub>3</sub>)  $\delta$  = 148.18–145.53 (m, 2Car), 146.48–143.90 (m, 2Car) 146.45 (d,  $J$  = 5.7 Hz, Car), 136.55 (s, Car), 129.32 (s, 2CHar), 128.85 (s, CHar), 128.66 (s, 2CHar), 127.75 (s, 2CHar), 118.81 (s, CHar), 117.27–116.91 (m, Car), 113.51 (s, 2CHar), 112.49–112.08 (m, Car), 63.59 (d,  $J$  = 7.0 Hz, OCH<sub>2</sub>), 62.45 (d,  $J$  = 7.4 Hz, OCH<sub>2</sub>), 50.62 (d,  $J$  = 157.1 Hz, CH), 39.14 (s, ArCH<sub>2</sub>S), 24.93 (d,  $J$  = 6.9 Hz, ArCH<sub>2</sub>), 16.56, 16.51, 16.48, and 16.42 (2CH<sub>3</sub>). HRMS (ESI<sup>+</sup>) calcd for C<sub>25</sub>H<sub>27</sub>F<sub>4</sub>NO<sub>3</sub>PS (M + H)<sup>+</sup>: 528.1385, found: 528.1387.

**4.1.2.9 Diethyl (2-(4-(decylthio)-2,3,5,6-tetrafluorophenyl)-1-(phenylamino)ethyl)phosphonate (2i).** Yellow oil (25 mg, 36%).





$^1\text{H}$  NMR (400 MHz,  $\text{CDCl}_3$ )  $\delta$  = 7.07–7.03 (m, 2H, 2CHar), 6.64 (t,  $J$  = 7.3 Hz, 1H, CHar), 6.53 (d,  $J$  = 7.9 Hz, 2H, 2CHar), 4.18–4.01 (m, 5H, CHP, 2OCH<sub>2</sub>), 3.82–3.79 (m, 1H, NH), 3.28–3.24 (m, 1H, ArCH<sub>2</sub>), 3.17–3.14 (m, 1H, ArCH<sub>2</sub>), 2.80 (t,  $J$  = 7.3 Hz, 2H, CH<sub>2</sub>S), 1.48–1.19 (m, 22H, 2CH<sub>3</sub>, CH<sub>3</sub>(CH<sub>2</sub>)<sub>8</sub>), 0.88 (t,  $J$  = 6.9 Hz, 3H, CH<sub>3</sub>(CH<sub>2</sub>)<sub>9</sub>).  $^{19}\text{F}$  NMR (377 MHz,  $\text{CDCl}_3$ )  $\delta$  = –134.89 (dd,  $J$  = 24.3, 12.0 Hz, 2F), –143.26 (dd,  $J$  = 24.3, 12.1 Hz, 2F).  $^{31}\text{P}$  NMR (162 MHz,  $\text{CDCl}_3$ )  $\delta$  = 23.52 (s).  $^{13}\text{C}$  NMR (101 MHz,  $\text{CDCl}_3$ )  $\delta$  = 148.15–145.53 (m, 2Car), 146.68–143.97 (m, 2Car), 146.41 (d,  $J$  = 6.9 Hz, Car), 129.27 (s, 2CHar), 118.76 (s, CHar), 116.81–116.44 (m, Car), 113.44 (s, 2CHar), 113.15 (s, Car), 63.67 (d,  $J$  = 7.0 Hz, OCH<sub>2</sub>), 62.46 (d,  $J$  = 7.4 Hz, OCH<sub>2</sub>), 50.61 (d,  $J$  = 157.7 Hz, CH), 34.84 (s, SCH<sub>2</sub>), 32.01 (s, CH<sub>3</sub>(CH<sub>2</sub>)<sub>8</sub>), 29.83 (s, CH<sub>3</sub>(CH<sub>2</sub>)<sub>8</sub>), 29.63 (s, CH<sub>3</sub>(CH<sub>2</sub>)<sub>8</sub>), 29.59 (s, CH<sub>3</sub>(CH<sub>2</sub>)<sub>8</sub>), 29.41 (s, CH<sub>3</sub>(CH<sub>2</sub>)<sub>8</sub>), 29.16 (s, CH<sub>3</sub>(CH<sub>2</sub>)<sub>8</sub>), 28.48 (s, CH<sub>3</sub>(CH<sub>2</sub>)<sub>8</sub>), 25.03 (d,  $J$  = 7.3 Hz, ArCH<sub>2</sub>), 22.80 (s, CH<sub>3</sub>(CH<sub>2</sub>)<sub>8</sub>), 16.59, 16.53, 16.49, and 16.43 (2CH<sub>3</sub>), 14.23 (s, CH<sub>3</sub>(CH<sub>2</sub>)<sub>9</sub>) ppm. HRMS ( $\text{ESI}^+$ ) calcd for  $\text{C}_{28}\text{H}_{41}\text{F}_4\text{N}_3\text{O}_3\text{P}$  ( $\text{M} + \text{H}$ )<sup>+</sup>: 578.2481, found: 578.2477.

**4.1.2.10 Methyl 2-acetamido-3-((4-(2-(diethoxyphosphoryl)-2-(phenylamino)ethyl)-2,3,5,6-tetrafluorophenyl)thio)propanoate (2j).** Yellow oil (49 mg, 71%).  $^1\text{H}$  NMR (400 MHz,  $\text{CDCl}_3$ )  $\delta$  = 7.06 (t,  $J$  = 7.7 Hz, 2H, 2CHar), 6.65 (t,  $J$  = 7.2 Hz, 1H, CHar), 6.54–6.51 (m, 2H, 2CHar), 6.38–6.34 (m, 1H, NHCO), 4.76–4.72 (m, 1H, CHN), 4.14–4.08 (m, 5H, CHP, 2OCH<sub>2</sub>), 3.86, 3.85 (2d,  $J$  = 3.6, 3.6 Hz, 1H, ArNH), 3.44, 3.41 (2s, 3H, CH<sub>3</sub>O), 3.35–3.14 (m, 4H, ArCH<sub>2</sub>, SCH<sub>2</sub>), 1.92 (s, 3H, CH<sub>3</sub>CO), 1.29 (t,  $J$  = 7.1 Hz, 3H, CH<sub>3</sub>), 1.17 (td,  $J$  = 7.1, 3.4 Hz, 3H, CH<sub>3</sub>).  $^{19}\text{F}$  NMR (377 MHz,  $\text{CDCl}_3$ )  $\delta$  = –133.64 to –133.74 (m, 2F), –142.36 to –142.49 (m, 2F) ppm.  $^{31}\text{P}$  NMR (162 MHz,  $\text{CDCl}_3$ )  $\delta$  = 23.45 and 23.41 (2s).  $^{13}\text{C}$  NMR (101 MHz,  $\text{CDCl}_3$ )  $\delta$  = 170.28 (s, CO), 169.92, 169.90 (2s, CO), 148.16–145.56 (m, 2Car), 146.31, 146.29 (2d,  $J$  = 5.0, 4.8 Hz, Car), 145.71–144.24 (m, 2Car), 129.34 (s, 2CHar), 118.86, 118.83 (2s, CHar), 118.10–117.59 (m, Car), 113.51, 113.44 (2s, 2CHar), 111.81–111.40 (m, Car), 63.6 (d,  $J$  = 7.0 Hz, POCH<sub>2</sub>), 62.56, 62.48 (2d,  $J$  = 7.5, 7.4 Hz, POCH<sub>2</sub>), 52.56, 52.55 (2s, CH<sub>3</sub>O), 52.08, 52.02 (2s, CHCH<sub>2</sub>S), 50.5, 50.4 (2d,  $J$  = 156.1, 156.2 PCH), 36.31, 36.24 (2t,  $J$  = 2.2, 2.1 Hz, SCH<sub>2</sub>), 24.89, 24.82 (2d,  $J$  = 5.1, 6.2 Hz, ArCH<sub>2</sub>), 22.95 (s, COCH<sub>3</sub>), 16.5, 16.4 (2d,  $J$  = 5.3, 5.7 Hz, CH<sub>3</sub>). HRMS ( $\text{ESI}^+$ ) calcd for  $\text{C}_{24}\text{H}_{30}\text{F}_4\text{N}_2\text{O}_6\text{PS}$  ( $\text{M} + \text{H}$ )<sup>+</sup>: 581.1498, found: 581.1503.

**4.1.3 General procedure for the nucleophilic aromatic substitution of 1a with amines.** To the mixture of **1a** (0.05 g, 0.12 mmol) in dry DMSO (1 mL), amine (3.6 mmol) was added under N<sub>2</sub> atmosphere in a Radley's tube. The mixture was stirred at 80 °C for 3 h. After cooling to the room temperature, the reaction mixture was poured into water (10 mL) and Et<sub>2</sub>O (10 mL). The aqueous phase was extracted with Et<sub>2</sub>O (3 × 10 mL), then combined organic layers were washed with water (3 × 20 mL) and dried over MgSO<sub>4</sub>. After filtration, solvent was removed under reduced pressure and the crude was purified by column chromatography (cyclohexane/AcOEt 1 : 1, v/v).

**4.1.3.1 Diethyl (1-(phenylamino)-2-(2,3,5,6-tetrafluoro-4-(methylamino)phenyl)ethyl)phosphonate (2k).** Pale yellow solid (31 mg, 60%), mp = 74–76 °C.  $^1\text{H}$  NMR (400 MHz,  $\text{CDCl}_3$ )  $\delta$  = 7.10–7.06 (m, 2H, 2CHar), 6.65 (t,  $J$  = 7.4 Hz, 1H, CHar), 6.55 (d,  $J$  = 7.9 Hz, 2H, 2CHar), 4.17–3.97 (m, 5H, CH, 2OCH<sub>2</sub>), 3.77 (dd,  $J$  = 10.6, 3.4 Hz, 1H, NH), 3.66 (bs, 1H, NH), 3.19–3.13 (m, 1H,

ArCH<sub>2</sub>), 3.06–2.99 (m, 4H, NCH<sub>3</sub>, ArCH<sub>2</sub>), 1.30 (t,  $J$  = 7.0 Hz, 3H, CH<sub>3</sub>), 1.20 (t,  $J$  = 7.1 Hz, 3H, CH<sub>3</sub>).  $^{19}\text{F}$  NMR (377 MHz,  $\text{CDCl}_3$ )  $\delta$  = –146.46 to –146.55 (m, 2F), –161.22 to –161.30 (m, 2F).  $^{31}\text{P}$  NMR (162 MHz,  $\text{CDCl}_3$ )  $\delta$  = 24.13 (s).  $^{13}\text{C}$  NMR (101 MHz,  $\text{CDCl}_3$ )  $\delta$  = 147.18–144.46 (m, 2Car), 146.75 (d,  $J$  = 5.9 Hz, Car), 138.76–136.11 (m, 2Car), 129.22 (s, 2CHar), 124.77–124.68 (m, Car), 118.42 (s, CHar), 113.48 (s, 2CHar), 103.17–102.67 (m, Car), 63.44 (d,  $J$  = 7.0 Hz, OCH<sub>2</sub>), 62.34 (d,  $J$  = 7.5 Hz, OCH<sub>2</sub>), 51.06 (d,  $J$  = 156.3 Hz, CH), 33.18 (s, NCH<sub>3</sub>), 24.03 (d,  $J$  = 6.6 Hz, ArCH<sub>2</sub>), 16.60, 16.55, 16.52, 16.46 (2CH<sub>3</sub>). HRMS ( $\text{ESI}^+$ ) calcd for  $\text{C}_{19}\text{H}_{24}\text{F}_4\text{N}_2\text{O}_3\text{P}$  ( $\text{M} + \text{H}$ )<sup>+</sup>: 435.1461, found: 435.1465.

**4.1.3.2 Diethyl (1-(phenylamino)-2-(2,3,5,6-tetrafluoro-4-(propylamino)phenyl)ethyl)phosphonate (2l).** Pale yellow solid (40 mg, 74%), mp = 78–80 °C.  $^1\text{H}$  NMR (400 MHz,  $\text{CDCl}_3$ )  $\delta$  = 7.08–7.04 (m, 1H, 2CHar), 6.64 (t,  $J$  = 7.3 Hz, 1H, CHar), 6.54 (d,  $J$  = 7.9 Hz, 2H, 2CHar), 4.17–3.98 (m, 5H, CH, 2OCH<sub>2</sub>), 3.80–3.65 (m, 1H, NH), 3.65 (s, 1H, CH<sub>2</sub>NH), 3.27–3.22 (m, 2H, CH<sub>3</sub>CH<sub>2</sub>CH<sub>2</sub>N), 3.18–3.13 (m, 1H, ArCH<sub>2</sub>), 3.06–3.00 (m, 1H, ArCH<sub>2</sub>), 1.52 (dd,  $J$  = 14.4, 7.2 Hz, 2H, CH<sub>3</sub>CH<sub>2</sub>CH<sub>2</sub>N), 1.30 (t,  $J$  = 7.1 Hz, 3H, CH<sub>3</sub>), 1.20 (t,  $J$  = 7.1 Hz, 3H, CH<sub>3</sub>), 0.92 (t,  $J$  = 7.4 Hz, 3H, CH<sub>3</sub>CH<sub>2</sub>CH<sub>2</sub>N).  $^{19}\text{F}$  NMR (377 MHz,  $\text{CDCl}_3$ )  $\delta$  = –146.46 to –146.53 (m, 2F), –160.68 to –160.72 (m, 2F).  $^{31}\text{P}$  NMR (162 MHz,  $\text{CDCl}_3$ )  $\delta$  = 24.13 (s).  $^{13}\text{C}$  NMR (101 MHz,  $\text{CDCl}_3$ )  $\delta$  = 147.16–144.51 (m, 2Car), 146.72 (d,  $J$  = 6.3 Hz, Car), 138.79–136.16 (m, 2Car), 129.17 (s, 2CHar), 127.17–126.90 (m, Car), 118.37 (s, CHar), 113.42 (s, 2CHar), 103.16–102.64 (m, Car), 63.45 (d,  $J$  = 7.0 Hz, OCH<sub>2</sub>), 62.31 (d,  $J$  = 7.5 Hz, OCH<sub>2</sub>), 51.03 (d,  $J$  = 156.8 Hz, CH), 47.82 (t,  $J$  = 4.0 Hz, CH<sub>3</sub>CH<sub>2</sub>CH<sub>2</sub>N), 24.04 (d,  $J$  = 7.0 Hz, ArCH<sub>2</sub>), 23.93 (s, CH<sub>3</sub>CH<sub>2</sub>CH<sub>2</sub>N), 16.57, 16.52, 16.49, and 16.43 (2CH<sub>3</sub>), 11.17 (s, CH<sub>3</sub>CH<sub>2</sub>CH<sub>2</sub>N). HRMS ( $\text{ESI}^+$ ) calcd for  $\text{C}_{21}\text{H}_{28}\text{F}_4\text{N}_2\text{O}_3\text{P}$  ( $\text{M} + \text{H}$ )<sup>+</sup>: 463.1774, found: 463.1773.

**4.1.3.3 Diethyl (2-(4-(butylamino)-2,3,5,6-tetrafluorophenyl)-1-(phenylamino)ethyl)phosphonate (2m).** Yellow oil (40 mg, 71%).  $^1\text{H}$  NMR (400 MHz,  $\text{CDCl}_3$ )  $\delta$  = 7.06 (t,  $J$  = 7.9 Hz, 2H, 2CHar), 6.64 (t,  $J$  = 7.3 Hz, 1H, CHar), 6.54 (d,  $J$  = 7.9 Hz, 2H, 2CHar), 4.17–3.97 (m, 5H, CH, 2OCH<sub>2</sub>), 3.78 (dd,  $J$  = 10.8, 3.1 Hz, 1H, NH), 3.60 (bs, 1H, NH), 3.31–3.25 (m, 2H, NCH<sub>2</sub>), 3.18–3.13 (m, 1H, ArCH<sub>2</sub>), 3.06–3.00 (m, 1H, ArCH<sub>2</sub>), 1.49–1.28 (m, 7H, CH<sub>3</sub>, CH<sub>2</sub>CH<sub>2</sub>), 1.20 (t,  $J$  = 7.1 Hz, 3H, CH<sub>3</sub>), 0.92 (t,  $J$  = 7.3 Hz, 3H, CH<sub>3</sub>(CH<sub>2</sub>)<sub>3</sub>).  $^{19}\text{F}$  NMR (377 MHz,  $\text{CDCl}_3$ )  $\delta$  = –146.45 to –146.52 (m, 2F), –160.68 to –160.72 (m, 2F).  $^{31}\text{P}$  NMR (162 MHz,  $\text{CDCl}_3$ )  $\delta$  = 24.13 (s) ppm.  $^{13}\text{C}$  NMR (101 MHz,  $\text{CDCl}_3$ )  $\delta$  = 147.16–146.70 (m, 2Car), 146.73 (d,  $J$  = 6.2 Hz, Car), 138.77–136.15 (m, 2Car), 129.18 (s, 2CHar), 127.20–126.97 (m, Car), 118.38 (s, CHar), 113.43 (s, 2CHar), 103.13–102.61 (m, Car), 63.45 (d,  $J$  = 7.0 Hz, OCH<sub>2</sub>), 62.31 (d,  $J$  = 7.5 Hz, OCH<sub>2</sub>), 51.05 (d,  $J$  = 156.8 Hz, CH), 45.82 (t,  $J$  = 4.0 Hz, NCH<sub>2</sub>), 32.88 (s, CH<sub>2</sub>CH<sub>2</sub>CH<sub>2</sub>), 24.04 (d,  $J$  = 6.7 Hz, ArCH<sub>2</sub>), 19.88 (s, CH<sub>3</sub>CH<sub>2</sub>CH<sub>2</sub>), 16.58, 16.52, 16.49, and 16.43 (2CH<sub>3</sub>), 13.87 (s, CH<sub>3</sub>(CH<sub>2</sub>)<sub>3</sub>). HRMS ( $\text{ESI}^+$ ) calcd for  $\text{C}_{22}\text{H}_{30}\text{F}_4\text{N}_2\text{O}_3\text{P}$  ( $\text{M} + \text{H}$ )<sup>+</sup>: 477.1930, found: 477.1932.

**4.1.3.4 Diethyl (2-(4-(allylamino)-2,3,5,6-tetrafluorophenyl)-1-(phenylamino)ethyl)phosphonate (2n).** Pale yellow oil (35 mg, 65%).  $^1\text{H}$  NMR (400 MHz,  $\text{CDCl}_3$ )  $\delta$  = 7.09–7.05 (m, 2H, 2CHar), 6.64 (t,  $J$  = 7.3 Hz, 1H, CHar), 6.54 (d,  $J$  = 7.9 Hz, 2H, 2CHar), 5.88–5.81 (m, 1H, CH<sub>2</sub>=CH), 5.15 (ddd,  $J$  = 13.7, 11.5, 1.3 Hz, 2H, CH<sub>2</sub>=CH), 4.17–4.02 (m, 5H, CHP, 2OCH<sub>2</sub>), 3.89–3.88 (m,



2H, NCH<sub>2</sub>), 3.77–3.76 (m, 2H, 2 NH), 3.20–3.14 (m, 1H, ArCH<sub>2</sub>), 3.07–2.97 (m, 1H, ArCH<sub>2</sub>), 1.30 (t, *J* = 7.1 Hz, 3H, CH<sub>3</sub>), 1.20 (t, *J* = 7.1 Hz, 3H, CH<sub>3</sub>). <sup>19</sup>F NMR (377 MHz, CDCl<sub>3</sub>) δ = −146.13 to −146.22 (m, 2F), −159.83 to −159.92 (m, 2F). <sup>31</sup>P NMR (162 MHz, CDCl<sub>3</sub>) δ = 24.08 (s). <sup>13</sup>C NMR (101 MHz, CDCl<sub>3</sub>) δ = 147.14–146.66 (m, 2Car), 146.70 (d, *J* = 6.3 Hz, Car), 138.93–136.29 (m, 2Car), 135.27 (s, CH<sub>2</sub>=CH), 129.20 (s, 2CHar), 126.66–126.39 (m, Car), 118.42 (s, CHar), 116.86 (s, CH<sub>2</sub>=CH), 113.43 (s, 2CHar), 103.89–103.38 (m, Car), 63.50 (t, *J* = 6.8 Hz, OCH<sub>2</sub>), 62.37 (t, *J* = 8.9 Hz, OCH<sub>2</sub>), 51.01 (d, *J* = 156.8 Hz, CHP), 48.35 (t, *J* = 4.3 Hz, NCH<sub>2</sub>), 24.09 (d, *J* = 7.0 Hz, ArCH<sub>2</sub>), 16.58, 16.52, 16.49, 16.43 (2CH<sub>3</sub>). HRMS (ESI<sup>+</sup>) calcd for C<sub>21</sub>H<sub>26</sub>F<sub>4</sub>N<sub>2</sub>O<sub>3</sub>P (M + H)<sup>+</sup>: 461.1617, found: 461.1616.

**4.1.3.5 Diethyl (1-(phenylamino)-2-(2,3,5,6-tetrafluoro-4-(methylamino)phenyl)ethyl)phosphonate (2o).** Pale yellow oil (38 mg, 63%). <sup>1</sup>H NMR (400 MHz, acetone-*d*<sub>6</sub>) δ = 7.33–7.27 (m, 5H, 5 CHar), 7.04–7.00 (m, 2H, 2CHar), 6.67–6.65 (m, 2H, 2CHar), 6.57 (t, *J* = 7.3 Hz, 1H, CHar), 5.60 (bs, 1H, NHCH<sub>2</sub>), 4.71–4.67 (m, 1H, NH), 4.52 (d, *J* = 7.0 Hz, 2H, NCH<sub>2</sub>), 4.08–4.01 (m, 5H, CH, 2OCH<sub>2</sub>), 3.16–3.10 (m, 1H, ArCH<sub>2</sub>), 3.00–2.90 (m, 1H, ArCH<sub>2</sub>), 1.21 (t, *J* = 7.1 Hz, 3H, CH<sub>3</sub>), 1.15 (t, *J* = 7.0 Hz, 3H, CH<sub>3</sub>). <sup>19</sup>F NMR (377 MHz, acetone-*d*<sub>6</sub>) δ = −147.27 to −147.39 (m, 2F), −161.21 to −161.32 (m, 2F). <sup>31</sup>P NMR (162 MHz, acetone-*d*<sub>6</sub>) δ = 23.69 (s). <sup>13</sup>C NMR (101 MHz, CDCl<sub>3</sub>) δ = 146.91–144.51 (m, 2Car), 146.69 (d, *J* = 6.0 Hz, Car), 139.10 (s, Car), 138.95–136.33 (m, 2Car), 129.23 (s, 2CHar), 128.89 (s, 2CHar), 127.81 (s, CHar), 127.67 (s, 2CHar), 126.72–126.57 (m, Car), 118.45 (s, CHar), 113.47 (s, 2CHar), 104.00–103.63 (m, Car), 63.47 (d, *J* = 7.0 Hz, OCH<sub>2</sub>), 62.33 (d, *J* = 7.5 Hz, OCH<sub>2</sub>), 51.01 (d, *J* = 156.0 Hz, CH), 50.18 (s, ArCH<sub>2</sub>N), 24.09 (d, *J* = 7.1 Hz, ArCH<sub>2</sub>), 16.58, 16.53, 16.49, 16.43 (2 × CH<sub>3</sub>). HRMS (ESI<sup>+</sup>) calcd for C<sub>25</sub>H<sub>28</sub>F<sub>4</sub>N<sub>2</sub>O<sub>3</sub>P (M + H)<sup>+</sup>: 511.1774, found: 511.1774.

**4.1.4 General procedure for the nucleophilic aromatic substitution of 1a with phenols.** To the mixture of phenol (0.18 mmol) and K<sub>2</sub>CO<sub>3</sub> (0.025 g, 0.18 mmol) in dry DMF (1 mL), a solution of **1a** (0.05 g, 0.12 mmol) in dry DMF (1 mL) was added under N<sub>2</sub> atmosphere in a Radley's tube. The mixture was stirred at 80 °C for 24 h. After cooling to the room temperature, the reaction mixture was poured into water (10 mL) and Et<sub>2</sub>O (10 mL). The aqueous phase was extracted with Et<sub>2</sub>O (3 × 10 mL), then combined organic layers were washed with water (3 × 20 mL) and dried over MgSO<sub>4</sub>. After filtration, solvent was removed under reduced pressure and the crude was purified by column chromatography (cyclohexane/AcOEt 1 : 1, v/v).

**4.1.4.1 Diethyl (1-(phenylamino)-2-(2,3,5,6-tetrafluoro-4-phenoxyphenyl)ethyl)phosphonate (2p).** Yellow oil (40 mg, 68%). <sup>1</sup>H NMR (400 MHz, CD<sub>3</sub>C(O)CD<sub>3</sub>) δ = 7.39–7.35 (m, 2H, 2CHar), 7.17–7.10 (m, 1H, CHar), 7.07–7.05 (m, 2H, 2CHar), 6.81 (d, *J* = 8.2 Hz, 2H, 2CHar), 6.72 (d, *J* = 7.9 Hz, 2H, 2CHar), 6.65 (t, *J* = 7.3 Hz, 1H, CHar), 4.84–4.82 (m, 1H, NH), 4.19–4.09 (m, 5H, CH, 2OCH<sub>2</sub>), 3.33–3.30 (m, 1H, ArCH<sub>2</sub>), 3.21–3.12 (m, 1H, ArCH<sub>2</sub>), 1.29 (t, *J* = 7.1 Hz, 3H, CH<sub>3</sub>), 1.22 (t, *J* = 7.2 Hz, 3H, CH<sub>3</sub>). <sup>19</sup>F NMR (377 MHz, CDCl<sub>3</sub>) δ = −143.74 to −143.83 (m, 2F), −154.95 to −155.03 (m, 2F). <sup>31</sup>P NMR (162 MHz, CD<sub>3</sub>C(O)CD<sub>3</sub>) δ = 23.02 (s). <sup>13</sup>C NMR (101 MHz, CDCl<sub>3</sub>) δ = 157.27 (s, Car), 147.14–144.45 (m, 2Car), 146.50 (d, *J* = 8.0 Hz, Car), 142.77–

140.05 (m, 2Car) 132.48–132.17 (m, Car), 129.83 (s, 2CHar), 129.37 (s, 2CHar), 123.61 (s, CHar), 118.66 (s, CHar), 115.38 (s, 2CHar), 113.17 (s, 2CHar), 112.74–112.23 (m, Car), 63.82 (d, *J* = 7.0 Hz, OCH<sub>2</sub>), 62.55 (d, *J* = 7.4 Hz, OCH<sub>2</sub>), 50.53 (d, *J* = 159.1 Hz, CH), 24.75 (d, *J* = 7.8 Hz, ArCH<sub>2</sub>), 16.63, 16.57, 16.55 and 16.49 (2CH<sub>3</sub>). HRMS (ESI<sup>+</sup>) calcd for C<sub>24</sub>H<sub>25</sub>F<sub>4</sub>NO<sub>4</sub>P (M + H)<sup>+</sup>: 498.1457, found: 498.1459.

**4.1.4.2 Diethyl (1-(phenylamino)-2-(2,3,5,6-tetrafluoro-4-(4-methoxyphenoxy)phenyl)ethyl)phosphonate (2q).** Yellow solid (30 mg, 48%), mp = 97–99 °C. <sup>1</sup>H NMR (400 MHz, CD<sub>3</sub>C(O)CD<sub>3</sub>) δ = 7.08–7.01 (m, 2H, 2CHar), 6.92–6.88 (m, 2H, 2CHar), 6.78–6.76 (m, 2H, 2CHar), 6.72–6.69 (m, 2H, 2CHar), 6.65 (t, *J* = 7.4 Hz, 1H, CHar), 4.83–4.80 (m, 1H, NH), 4.16–4.09 (m, 5H, CH, 2OCH<sub>2</sub>), 3.78 (s, 3H, OCH<sub>3</sub>), 3.33–3.27 (m, 1H, ArCH<sub>2</sub>), 3.19–3.10 (m, 1H, ArCH<sub>2</sub>), 1.30–1.26 (m, 3H, CH<sub>3</sub>), 1.24–1.15 (m, 3H, CH<sub>3</sub>). <sup>19</sup>F NMR (377 MHz, CDCl<sub>3</sub>) δ = −143.91 to −144.00 (m, 2F), −155.33 to −155.42 (m, 2F). <sup>31</sup>P NMR (162 MHz, CDCl<sub>3</sub>) δ = 23.42 (s). <sup>13</sup>C NMR (101 MHz, CDCl<sub>3</sub>) δ = 155.85 (s, Car), 151.42 (s, Car), 147.13–144.49 (m, 2Car) 146.51 (d, *J* = 7.9 Hz, Car), 142.78–140.10 (m, 2Car), 133.40–133.04 (m, Car) 129.36 (s, 2CHar), 118.64 (s, CHar), 116.70 (s, 2CHar), 114.79 (s, 2CHar), 113.21 (s, 2CHar), 112.34–111.83 (m, Car), 63.80 (d, *J* = 7.0 Hz, OCH<sub>2</sub>), 62.55 (d, *J* = 7.4 Hz, OCH<sub>2</sub>), 55.82 (s, OCH<sub>3</sub>), 50.57 (d, *J* = 158.7 Hz, CH), 24.70 (d, *J* = 7.6 Hz, ArCH<sub>2</sub>), 16.63, 16.58, 16.55, and 16.50 (2CH<sub>3</sub>). HRMS (ESI<sup>+</sup>) calcd for C<sub>25</sub>H<sub>27</sub>F<sub>4</sub>NO<sub>5</sub>P (M + H)<sup>+</sup>: 528.1563, found: 528.1567.

**4.1.4.3 Diethyl (2-(4-(4-chlorophenoxy)-2,3,5,6-tetrafluorophenyl)-1-(phenylamino)ethyl)phosphonate (2r).** Yellow solid (35 mg, 56%), mp = 94–99 °C. <sup>1</sup>H NMR (400 MHz, CD<sub>3</sub>C(O)CD<sub>3</sub>) δ = 7.40–7.38 (m, 2H, 2CHar), 7.08–7.02 (m, 2H, 2CHar), 6.85–6.83 (m, 2H, 2CHar), 6.72 (d, *J* = 7.9 Hz, 2H, 2CHar), 6.66 (t, *J* = 7.3 Hz, 1H, CHar), 4.87–4.83 (m, 1H, NH), 4.17–4.10 (m, 5H, CH, 2OCH<sub>2</sub>), 3.34–3.28 (m, 1H, ArCH<sub>2</sub>), 3.21–3.14 (m, 1H, ArCH<sub>2</sub>), 1.29 (t, *J* = 7.1 Hz, 3H, CH<sub>3</sub>), 1.22 (t, *J* = 7.1 Hz, 3H, CH<sub>3</sub>). <sup>19</sup>F NMR (377 MHz, CDCl<sub>3</sub>) δ = −143.37 to −143.45 (m, 2F), −154.94 to −155.02 (m, 2F). <sup>31</sup>P NMR (162 MHz, CDCl<sub>3</sub>) δ = 23.24 (s). <sup>13</sup>C NMR (101 MHz, CDCl<sub>3</sub>) δ = 155.79 (s, Car), 147.12–142.57 (m, 2Car), 146.47 (d, *J* = 8.1 Hz, Car), 142.57–139.85 (m, 2Car) 132.10–131.84 (m, Car), 129.77 (s, 2CHar), 129.36 (s, 2CHar), 128.73 (s, Car), 118.59 (s, CHar), 116.75 (s, 2CHar), 113.07 (s, 2CHar), 112.95–112.80 (m, Car), 63.87 (d, *J* = 7.0 Hz, OCH<sub>2</sub>), 62.59 (d, *J* = 7.5 Hz, OCH<sub>2</sub>), 50.38 (d, *J* = 159.4 Hz, CH), 24.74 (d, *J* = 7.9 Hz, ArCH<sub>2</sub>), 16.62, 16.57, 16.55, and 16.49 (2CH<sub>3</sub>) ppm. HRMS (ESI<sup>+</sup>) calcd for C<sub>24</sub>H<sub>24</sub>ClF<sub>4</sub>NO<sub>4</sub>P (M + H)<sup>+</sup>: 532.1068, found: 532.1066.

**4.1.4.4 Diethyl (1-(phenylamino)-2-(2,3,5,6-tetrafluoro-4-(3-nitrophenoxy)phenyl)ethyl)phosphonate (2s).** Yellow solid (31 mg, 48%), mp = 77–79 °C. <sup>1</sup>H NMR (400 MHz, CD<sub>3</sub>C(O)CD<sub>3</sub>) δ = 8.05 (ddd, *J* = 8.2, 2.1, 0.8 Hz, 1H, CHar), 7.84 (t, *J* = 2.3 Hz, 1H, CHar), 7.71 (t, *J* = 8.3 Hz, 1H, CHar), 7.24 (dd, *J* = 8.3, 2.6 Hz, 1H, CHar), 7.10–7.06 (m, 2H, 2CHar), 6.74 (d, *J* = 7.9 Hz, 2H, 2CHar), 6.63 (t, *J* = 7.3 Hz, 1H, CHar), 4.86 (d, *J* = 13.7 Hz, 1H, NH), 4.17–4.10 (m, 5H, CH, 2OCH<sub>2</sub>), 3.35–3.30 (m, 1H, ArCH<sub>2</sub>), 3.23–3.14 (m, 1H, ArCH<sub>2</sub>), 1.28 (t, *J* = 7.1 Hz, 3H, CH<sub>3</sub>), 1.22 (t, *J* = 7.1 Hz, 3H, CH<sub>3</sub>). <sup>19</sup>F NMR (377 MHz, CDCl<sub>3</sub>) δ = −142.44 (dd, *J* = 22.6, 9.4 Hz, 2F), −154.52 to −154.61 (dd, *J* = 22.0, 9.3 Hz, 2F). <sup>31</sup>P NMR (162 MHz, CDCl<sub>3</sub>) δ = 23.25 (s). <sup>13</sup>C NMR (101 MHz, CDCl<sub>3</sub>) δ = 157.42 (s, Car), 149.36 (s, Car),



RSC Adv., 2019, 9, 24117–24133 | 24131



method of choice to determine cell reproductive death after treatment with ionizing radiation, but can also be used to determine effectiveness of other cytotoxic agents. Only a fraction of seeded cell retains the capacity to product colonies. The protocol was adapted from literature methods.<sup>64</sup> T98G and HaCaT cells were seeded in 6-well tissue culture plates at a density of 500 cells per well according to the morphology and growth patterns of each cell line, and were allowed adhere for 24 hours before treatment. The cells were treated with different compound concentrations (2  $\mu$ M, 10  $\mu$ M, 20  $\mu$ M, 50  $\mu$ M, 100  $\mu$ M) for 7 days. Triplicate samples were used for each treatment. Medium containing the treatment was replaced with a compound-free medium after 24 h. Plates were rinsed in milliQ water and colonies were methanol-fixed and stained with 1% gentian violet and clones were counted under a light microscope.

**4.3.4 In silico pharmacokinetic prediction.** Calculations of pharmacokinetic profile descriptors of synthesized compounds were performed by various software solutions accessible online. The transformation of the stoichiometric formulas of the compounds into a SMILES code (Simplified Molecular Input Line Entry System) was carried out by ChemBioDraw Ultra version 12.0 program (Cambridge Software). The SMILES code was applied to calculate log *P* values (octanol/water partition coefficient), PSA (topological polar surface area) and aPSA (apolar surface area). The log *P* values were calculated by ALOGPS 2.1 software (<http://www.vcclab.org/lab/alogps>).<sup>65</sup> PSA and aPSA descriptors were calculated using the VEGA ZZ program (<http://www.vegazz.net>).<sup>66</sup> The pharmacokinetic profiles were also evaluated according to Lipinski's "rule of five"<sup>67</sup> by using Molinspiration application (<http://www.molinspiration.com>), which analyses molecular weight (MW), number of hydrogen-bond acceptors (HBA), and number of hydrogen-bond donors (HBD). The Caco-2 prediction model based on descriptors generated by preADMET (<http://preadmet.bmdrc.org>) was used to compute Caco-2 apparent permeability (*t*<sub>Papp</sub>), for the tested compounds. In this model a number of hydrogen bond donors and three molecular surface area properties determine membrane permeability of compounds.

## Conflicts of interest

There are no conflicts to declare.

## Acknowledgements

This research was supported in part by PL-Grid Infrastructure (<http://www.plgrid.pl/en>).

## References

- 1 Z.-Q. Zhu, L.-J. Xiao, D. Guo, X. Chen, J.-J. Ji, X. Zhu, Z.-B. Xi and Z.-G. Le, *J. Org. Chem.*, 2019, **84**, 435–442.
- 2 Z. Chen, P. Marce, R. Resende, P. M. Alzari, A. Carlos Frasc, J. M. H. van den Elsen, S. J. Crennell and A. G. Watts, *Eur. J. Med. Chem.*, 2018, **158**, 25–33.
- 3 V. M. S. Isca and A. C. Fernandes, *Green Chem.*, 2018, **20**, 3242–3245.
- 4 A. Mucha, P. Kafarski and Ł. Berlicki, *J. Med. Chem.*, 2011, **54**, 5955–5980.
- 5 X.-C. Huang, M. Wang, Y.-M. Pan, G.-Y. Yao, H.-S. Wang, X.-Y. Tian, J.-K. Qin and Y. Zhang, *Eur. J. Med. Chem.*, 2013, **69**, 508–520.
- 6 Q. Wang, L. Yang, H. Ding, X. Chen, H. Wang and X. Tang, *Bioorg. Chem.*, 2016, **69**, 132–139.
- 7 Z. Rezaei, H. Firouzabadi, N. Iranpoor, A. Ghaderi, M. R. Jafari, A. A. Jafari and H. R. Zare, *Eur. J. Med. Chem.*, 2009, **44**, 4266–4275.
- 8 I. Kraicheva, A. Bogomilova, I. Tsacheva, G. Momekov and K. Troev, *Eur. J. Med. Chem.*, 2009, **44**, 3363–3367.
- 9 Y.-C. Yu, W.-B. Kuang, R.-Z. Huang, Y.-L. Fang, Y. Zhang, Z.-F. Chen and X.-L. Ma, *MedChemComm*, 2017, **8**, 1158–1172.
- 10 B.-A. Song, Y.-L. Wu, S. Yang, D.-Y. Hu, X.-Q. He and L.-H. Jin, *Molecules*, 2003, **8**, 186–192.
- 11 F. R. Atherton, C. H. Hassall and R. W. Lambert, *J. Med. Chem.*, 1986, **29**, 29–40.
- 12 P. Kafarski and B. Lejczak, *Phosphorus, Sulfur Silicon Relat. Elem.*, 1991, **63**, 193–215.
- 13 F. Westheimer, *Science*, 1987, **235**, 1173–1178.
- 14 V. D. Romanenko and V. P. Kukhar, *Chem. Rev.*, 2006, **106**, 3868–3935.
- 15 S. A. Bernhard and L. E. Orgel, *Science*, 1959, **130**, 625–626.
- 16 K. V. Turcheniuk, V. P. Kukhar, G.-V. Röschenthaler, J. L. Aceña, V. A. Soloshonok and A. E. Sorochinsky, *RSC Adv.*, 2013, **3**, 6693–6716.
- 17 G. F. Makhaeva, A. Y. Aksinenko, V. B. Sokolov, I. I. Baskin, V. A. Palyulin, N. S. Zefirov, N. D. Hein, J. W. Kampf, S. J. Wijeyesakere and R. J. Richardson, *Chem.-Biol. Interact.*, 2010, **187**, 177–184.
- 18 E. P. Gillis, K. J. Eastman, M. D. Hill, D. J. Donnelly and N. A. Meanwell, *J. Med. Chem.*, 2015, **58**, 8315–8359.
- 19 B. E. Smart, *J. Fluorine Chem.*, 2001, **109**, 3–11.
- 20 S. L. Cobb and C. D. Murphy, *J. Fluorine Chem.*, 2009, **130**, 132–143.
- 21 L. D. Quin and G. S. Quin, *Comp. Biochem. Physiol., Part B: Biochem. Mol. Biol.*, 2001, **128**, 173–185.
- 22 M. Salwiczek, E. K. Nyakatura, U. I. M. Gerling, S. Ye and B. Koks, *Chem. Soc. Rev.*, 2012, **41**, 2135–2171.
- 23 D. M. Ryan, S. B. Anderson, F. T. Senguen, R. E. Youngman and B. L. Nilsson, *Soft Matter*, 2010, **6**, 475–479.
- 24 H. Zheng, K. Comeforo and J. Gao, *J. Am. Chem. Soc.*, 2009, **131**, 18–19.
- 25 C. J. Pace, H. Zheng, R. Mylvaganam, D. Kim and J. Gao, *Angew. Chem., Int. Ed.*, 2012, **51**, 103–107.
- 26 G. Akçay and K. Kumar, *J. Fluorine Chem.*, 2009, **130**, 1178–1182.
- 27 C. J. Pace and J. Gao, *Acc. Chem. Res.*, 2013, **46**, 907–915.
- 28 S. E. Wheeler and K. N. Houk, *J. Chem. Theory Comput.*, 2009, **5**, 2301–2312.
- 29 T. Siodla, W. P. Oziminski, M. Hoffmann, H. Koroniak and T. M. Krygowski, *J. Org. Chem.*, 2014, **79**, 7321–7331.





- 30 F. Wang, L. Qin, P. Wong and J. Gao, *Org. Lett.*, 2011, **13**, 236–239.
- 31 L. Qin, C. Sheridan and J. Gao, *Org. Lett.*, 2012, **14**, 528–531.
- 32 A. M. Spokoyny, Y. Zou, J. J. Ling, H. Yu, Y.-S. Lin and B. L. Pentelute, *J. Am. Chem. Soc.*, 2013, **135**, 5946–5949.
- 33 J. Kwiczak-Yiğitbaşı, J.-L. Pirat, D. Virieux, J.-N. Volle, A. Janiak, M. Hoffmann and D. Pluskota-Karwatka, *Arabian J. Chem.*, 2018, DOI: 10.1016/j.arabjc.2018.05.002.
- 34 A. Pawlowska, J.-N. Volle, D. Virieux, J.-L. Pirat, A. Janiak, M. Nowicki, M. Hoffmann and D. Pluskota-Karwatka, *Tetrahedron*, 2018, **74**, 975–986.
- 35 S. A. Azizi and C. Miyamoto, *J. NeuroVirol.*, 1998, **4**, 204–216.
- 36 J. D. Lathia, S. C. Mack, E. E. Mulkearns-Hubert, C. L. L. Valentim and J. N. Rich, *Genes Dev.*, 2015, **29**, 1203–1217.
- 37 P. Anja, J. Anahid and K. Janko, *Semin. Cancer Biol.*, 2018, **53**, 168–177.
- 38 M. Sivaparthi, R. Sawaya, S. W. Wang, A. Rayford, M. Yamamoto, L. A. Liotta, G. L. Nicolson and J. S. Rao, *Clin. Exp. Metastasis*, 1995, **13**, 49–56.
- 39 M. Sivaparthi, M. Yamamoto, G. L. Nicolson, Z. L. Gokaslan, G. N. Fuller, L. A. Liotta, R. Sawaya and J. S. Rao, *Clin. Exp. Metastasis*, 1996, **14**, 27–34.
- 40 G. F. Makhaeva, S. V. Lushchekina, O. G. Serebryakova, A. Y. Aksinenko, T. V. Goreva, R. J. Richardson and I. V. Martynov, *Dokl. Biochem. Biophys.*, 2013, **451**, 203–206.
- 41 M. Sieńczyk and J. Oleksyszyn, *Curr. Med. Chem.*, 2009, **16**, 1673–1687.
- 42 J. Ajenjo, M. Greenhall, C. Zarantonello and P. Beier, *Beilstein J. Org. Chem.*, 2016, **12**, 192–197.
- 43 I. A. Khalfina and V. M. Vlasov, *Russ. J. Org. Chem.*, 2005, **41**, 978–983.
- 44 C. S. Gutsche, M. Ortwerth, S. Gräfe, K. J. Flanagan, M. O. Senge, H.-U. Reissig, N. Kulak and A. Wiehe, *Chem.–Eur. J.*, 2016, **22**, 13953–13964.
- 45 A. Bondi, *J. Phys. Chem.*, 1964, **68**, 441–451.
- 46 C. A. Lipinski, *Adv. Drug Delivery Rev.*, 2016, **101**, 34–41.
- 47 C. A. Lipinski, F. Lombardo, B. W. Dominy and P. J. Feeney, *Adv. Drug Delivery Rev.*, 1997, **23**, 3–25.
- 48 D. F. Veber, S. R. Johnson, H.-Y. Cheng, B. R. Smith, K. W. Ward and K. D. Kopple, *J. Med. Chem.*, 2002, **45**, 2615–2623.
- 49 M. Yazdani, S. L. Glynn, J. L. Wright and A. Hawi, *Pharm. Res.*, 1998, **15**, 1490–1494.
- 50 X. Ma, C. Chen and J. Yang, *Acta Pharmacol. Sin.*, 2005, **26**, 500–512.
- 51 S. Lapointe, A. Perry and N. A. Butowski, *Lancet*, 2018, **392**, 432–446.
- 52 Q. T. Ostrom, L. Bauchet, F. G. Davis, I. Deltour, J. L. Fisher, C. E. Langer, M. Pekmezci, J. A. Schwartzbaum, M. C. Turner, K. M. Walsh, M. R. Wrensch and J. S. Barnholtz-Sloan, *Neuro-Oncology*, 2014, **16**, 896–913.
- 53 G. M. Sheldrick, *Acta Crystallogr., Sect. C: Struct. Chem.*, 2015, **71**, 3–8.
- 54 I. J. Bruno, J. C. Cole, P. R. Edgington, M. Kessler, C. F. Macrae, P. McCabe, J. Pearson and R. Taylor, *Acta Crystallogr., Sect. B: Struct. Sci.*, 2002, **58**, 389–397.
- 55 J.-D. Chai and M. Head-Gordon, *Phys. Chem. Chem. Phys.*, 2008, **10**, 6615–6620.
- 56 J. J. P. Stewart, *J. Comput. Chem.*, 1989, **10**, 209–220.
- 57 C. C. J. Roothaan, *Rev. Mod. Phys.*, 1951, **23**, 69–89.
- 58 J. B. Collins, P. von R. Schleyer, J. S. Binkley and J. A. Pople, *J. Chem. Phys.*, 1976, **64**, 5142–5151.
- 59 M. J. Frisch, G. W. Trucks, H. B. Schlegel, G. E. Scuseria, M. A. Robb, J. R. Cheeseman, G. Scalmani, V. Barone, G. A. Petersson, H. Nakatsuji, X. Li, M. Caricato, A. Marenich, J. Bloino, B. G. Janesko, R. Gomperts, B. Mennucci, H. P. Hratchian, J. V. Ortiz, A. F. Izmaylov, J. L. Sonnenberg, D. Williams-Young, F. Ding, F. Lipparini, F. Egidi, J. Goings, B. Peng, A. Petrone, T. Henderson, D. Ranasinghe, V. G. Zakrzewski, J. Gao, N. Rega, G. Zheng, W. Liang, M. Hada, M. Ehara, K. Toyota, R. Fukuda, J. Hasegawa, M. Ishida, T. Nakajima, Y. Honda, O. Kitao, H. Nakai, T. Vreven, K. Throssell, J. A. Montgomery Jr, J. E. Peralta, F. Ogliaro, M. Bearpark, J. J. Heyd, E. Brothers, K. N. Kudin, V. N. Staroverov, T. Keith, R. Kobayashi, J. Normand, K. Raghavachari, A. Rendell, J. C. Burant, S. S. Iyengar, J. Tomasi, M. Cossi, J. M. Millam, M. Klene, C. Adamo, R. Cammi, J. W. Ochterski, R. L. Martin, K. Morokuma, O. Farkas, J. B. Foresman, and D. J. Fox, *Gaussian 09, Revision A.02*, Gaussian, Inc., Wallingford CT, 2016.
- 60 P. Atkins and J. de Paula, *Physical Chemistry*, W. H. Freeman, New York, 9th edn, 2009.
- 61 H. Shanan-Atidi and K. H. Bar-Eli, *J. Phys. Chem.*, 1970, **74**, 961–963.
- 62 K. Salus, M. Hoffmann, T. Siodła, B. Wyrzykiewicz and D. Pluskota-Karwatka, *New J. Chem.*, 2017, **41**, 2409–2424.
- 63 C. P. R. Xavier, C. F. Lima, M. Rohde and C. Pereira-Wilson, *Cancer Chemother. Pharmacol.*, 2011, **68**, 1449–1457.
- 64 L. C. Crowley, M. E. Christensen and N. J. Waterhouse, *Cold Spring Harb. Protoc.*, 2016, DOI: 10.1101/pdb.prot087171.
- 65 I. V. Tetko, J. Gasteiger, R. Todeschini, A. Mauri, D. Livingstone, P. Ertl, V. A. Palyulin, E. V. Radchenko, N. S. Zefirov, A. S. Makarenko, V. Yu. Tanchuk and V. V. Prokopenko, *J. Comput.-Aided Mol. Des.*, 2005, **19**, 453–463.
- 66 A. Pedretti, L. Villa and G. Vistoli, *J. Mol. Graphics Modell.*, 2002, **21**, 47–49.
- 67 C. A. Lipinski, F. Lombardo, B. W. Dominy and P. J. Feeney, *Adv. Drug Delivery Rev.*, 2001, **46**, 3–26.

